

NKTR-358: A novel regulatory T-cell stimulator that selectively stimulates expansion and suppressive function of regulatory T cells for the treatment of autoimmune and inflammatory diseases

Neha Dixit^a, Christie Fanton^a, John L. Langowski^{a,1}, Yolanda Kirksey^a, Peter Kirk^{a,2}, Thomas Chang^a, Janet Cetz^a, Vidula Dixit^{a,3}, Grace Kim^{a,4}, Peiwen Kuo^{a,5}, Mekhala Maiti^a, Yinyan Tang^a, Laurie A. VanderVeen^{a,5}, Ping Zhang^a, Myong Lee^a, Jerome Ritz^b, Yusuke Kamihara^{b,6}, Chunmei Ji^a, Werner Rubas^a, Theresa D. Sweeney^a, Stephen K. Doberstein^{a,7}, Jonathan Zalevsky^{a,*}

^a Nektar Therapeutics, 455 Mission Bay Boulevard South, San Francisco, CA, 94158, USA

^b Dana-Farber Cancer Institute, Harvard Medical School, 450 Brookline Avenue, Boston, MA, 02215, USA

ARTICLE INFO

Keywords:

Interleukin-2
IL-2 receptor
Systemic lupus erythematosus
Regulatory T cells
Autoimmune disease
Therapeutic

ABSTRACT

Impaired interleukin-2 (IL-2) production and regulatory T-cell dysfunction have been implicated as immunological mechanisms central to the pathogenesis of multiple autoimmune and inflammatory diseases. NKTR-358, a novel regulatory T-cell stimulator, is an investigational therapeutic that selectively restores regulatory T-cell homeostasis in these diseases. We investigated NKTR-358's selectivity for regulatory T-cells, receptor-binding properties, *ex vivo* and *in vivo* pharmacodynamics, ability to suppress conventional T-cell proliferation in mice and non-human primates, and functional activity in a murine model of systemic lupus erythematosus. *In vitro*, NKTR-358 demonstrated decreased affinity for IL-2R α , IL-2R β , and IL-2R $\alpha\beta$ compared with recombinant human IL-2 (rhIL-2). A single dose of NKTR-358 in cynomolgus monkeys produced a greater than 15-fold increase in regulatory T-cells, and the increase lasted until day 14, while daily rhIL-2 administration for 5 days only elicited a 3-fold increase, which lasted until day 7. Repeated dosing of NKTR-358 over 6 months in cynomolgus monkeys elicited cyclical, robust increases in regulatory T-cells with no loss in drug activity over the course of treatment. Regulatory T-cells isolated from NKTR-358-treated mice displayed a sustained, higher suppression of conventional T-cell proliferation than regulatory T-cells isolated from vehicle-treated mice. NKTR-358 treatment in a mouse model (MRL/MpJ-Fas^{lpr}) of systemic lupus erythematosus for 12 weeks maintained elevated regulatory T-cells for the treatment duration and ameliorated disease progression. Together, these results suggest that NKTR-358 has the ability to elicit sustained and preferential proliferation and activation of regulatory T-cells without corresponding effects on conventional T-cells, with improved pharmacokinetics compared with rhIL-2.

* Corresponding author.

E-mail addresses: ndixit@nektar.com (N. Dixit), cfanton@nektar.com (C. Fanton), heyski@yahoo.com (J.L. Langowski), ykirksey@nektar.com (Y. Kirksey), pbkirk@gmail.com (P. Kirk), tchang@nektar.com (T. Chang), jcetz@nektar.com (J. Cetz), vidula.67@yahoo.com (V. Dixit), g12acekim@gmail.com (G. Kim), peiwen.kuo@gmail.com (P. Kuo), mmaiti@nektar.com (M. Maiti), ytang@nektar.com (Y. Tang), laurie_vanderveen@yahoo.com (L.A. VanderVeen), pzhang@nektar.com (P. Zhang), mylee@nektar.com (M. Lee), jerome_ritz@dfci.harvard.edu (J. Ritz), ykamihar@east.ncc.go.jp (Y. Kamihara), cji@nektar.com (C. Ji), wrubas@nektar.com (W. Rubas), tsweeney@nektar.com (T.D. Sweeney), steve@kahilihohlo.com (S.K. Doberstein), jzalevsky@nektar.com (J. Zalevsky).

¹ Present address: Kite Pharma (a Gilead company), 2400 Broadway, Santa Monica, CA 90404, USA.

² Present address: Immunocore, 92 Park Drive, Milton Park, Abingdon, Oxfordshire, OX14 4RY, UK.

³ Present address: Bellicum, 611 Gateway Blvd, 820, South San Francisco, CA 94080, USA.

⁴ Present address: Verge Genomics, 2 Tower Place, South San Francisco, CA 94080, USA.

⁵ Present address: Gilead Sciences, 333 Lakeside Drive, Foster City, CA 94404, USA.

⁶ Present address: National Cancer Center Hospital East, 6-5-1 Kashiwanoha, Kashiwa, Chiba 277-8577, Japan.

⁷ Present address: Kahilihohlo Consulting, 129 Elsie Street, San Francisco, CA 94110, USA.

<https://doi.org/10.1016/j.jtauto.2021.100103>

Received 20 April 2021; Accepted 25 April 2021

Available online 6 May 2021

2589-9090/© 2021 The Authors.

Published by Elsevier B.V. This is an open access article under the CC BY-NC-ND license

(<http://creativecommons.org/licenses/by-nc-nd/4.0/>).

1. Introduction

The cytokine interleukin-2 (IL-2) plays a central role in both immunological antitumor activity and self-tolerance. IL-2 is a fundamental T-cell growth factor that is responsible for the survival, proliferation, and differentiation of conventional T cells (Tcons) [1]. Increased expression of IL-2 involves natural killer (NK) and effector T cells and is essential for the generation of productive immunity in response to infection or antitumor immune responses in the case of malignancy. However, IL-2 also plays a crucial role in promoting the development of a unique T-cell lineage called regulatory T cells (Tregs), which can originate in the thymus or be induced in the peripheral blood [2]. A key physiological function of Tregs is to promote immunological self-tolerance by suppressing autoreactive or tumor-reactive cytotoxic T lymphocytes (CTLs) and other T cells [3–5]. Tregs are capable of modulating the function of Tcons, maintaining immunological homeostasis, and preventing autoimmunity. Thus, while expansion of suppressive Tregs would be undesirable in cancer immunotherapy, the ability to drive Treg proliferation and activation could prove beneficial for patients with autoimmune and other inflammatory disorders, as a number of these conditions are associated with progressive disruption in the homeostatic balance of Tregs relative to Tcons [6]. In patients with systemic lupus erythematosus (SLE), for example, disease flares are associated with reduced numbers of circulating Tregs, loss of self-tolerance, and an increase in autoreactive antibodies [6,7].

The pleiotropic and context-specific effects of IL-2 can be attributed to its differential binding affinity for the members of the IL-2 receptor-signaling complex [8], which consists of combinations of IL-2R α (CD25), IL-2R β (CD122), and common γ -chain (CD132) receptors [3], as well as the differential expression of these IL-2 receptor subunits across various T-cell populations [2]. At high concentrations, IL-2 induces expansion of CD8⁺ effector T cells and memory CTLs, as well as NK cells, through the intermediate-affinity $\beta\gamma$ receptor [3]. This property gives high-dose IL-2 its antitumor activity and led to its development as one of the first immunotherapeutic treatments for cancer [9–11]. In contrast, Tregs are activated at low concentrations of IL-2 due to higher cell-surface expression of IL-2R α and enhanced downstream signaling associated with the trimeric IL-2R $\alpha\beta\gamma$ receptor complex [12].

Preliminary evidence of the clinical efficacy of low-dose recombinant human IL-2 (rhIL-2) in autoimmune conditions has been reported in multiple indications, including chronic graft-versus-host disease [13], vasculitis induced by the hepatitis C virus [14], SLE [15,16], and type 1 diabetes [17]. In a Phase I/IIa open-label clinical trial (TRANSREG), 46 patients, across 11 selected autoimmune diseases, received low-dose rhIL-2 for 6 months. Patients demonstrated significant improvement in arthralgia and chronic fatigue symptoms, indicating potential clinical benefit [18]. This study demonstrated specific Treg expansion and activation in all patients, irrespective of the underlying disease indication, without any effector T-cell activation. However, in all of these preliminary clinical studies, low-dose rhIL-2 only increased Treg populations by two- to five-fold [13–15,18]. A higher rhIL-2 dose to further increase Treg populations would be expected to also induce Tcons; hence, rhIL-2 has a narrow therapeutic window for use in autoimmune diseases. In addition, rhIL-2 also displays a suboptimal pharmacokinetic (PK) profile due to its short half-life [19]. The narrow therapeutic window, short elimination half-life, and need for frequent dosing of rhIL-2 have so far limited its practicality as a therapy for autoimmune diseases [19].

Polymer conjugation is a well-validated approach to alter and optimize the biological properties of macromolecules. Covalent attachment to polyethylene glycol (PEG) chains can, in some cases, not only alter a molecule's PK properties, but also its receptor binding properties [20]. We have previously reported our work with bempegaldesleukin (BEM-PEG; NKTR-214), a PEG conjugate of rhIL-2 [21,22], engineered to limit binding to the IL-2R α subunit thereby promoting preferential signaling to the dimeric IL-2R $\beta\gamma$. Consequently, BEMPEG increases the

proliferation, activation, and effector function of CD8⁺ T cells and NK cells within the tumor microenvironment without expanding the undesirable intratumoral Treg cells [20]. Here, we have used our experience with polymer conjugation and our understanding of IL-2 biology to create NKTR-358, a stable PEG conjugate of rhIL-2 designed to selectively favor Treg activation and proliferation with minimal effects on Tcons. In the present study, we demonstrate by a variety of measures that NKTR-358 can induce sustained, selective proliferation and activation of Tregs without stimulating Tcon cells, and that it has improved PD compared with multiple doses of rhIL-2. NKTR-358 demonstrated increased functional activity of Tregs in an *ex-vivo* suppression assay and was associated with improvement in several pathologies associated with disease progression in a murine model of SLE.

2. Materials and methods

2.1. Reagents

NKTR-358 is a PEGylated form of rhIL-2, which has the same amino acid sequence as aldesleukin (des-alanyl-1, serine-125 human interleukin-2, Proleukin®). rhIL-2 (aldesleukin) was manufactured by Althea Ajinomoto (San Diego, CA) and diluted in product formulation buffer (5% dextrose) as recommended by the manufacturer. The rhIL-2 was conjugated to polyethylene glycol (PEG) chains by stable covalent bonds and the PEG reagent was manufactured at Nektar. rhIL-2 was reacted with a 10-fold molar excess of Nektar PEG reagent and the product was purified from the reaction mixture using cation exchange chromatography. The purified NKTR-358 drug product was concentrated by a diafiltration step and then formulated as a liquid solution in 10 mM sodium acetate, 200 mM sodium chloride, 2% sucrose, pH 5, prepared in sterile water for injection.

For *in vivo* murine studies, rhIL-2 and NKTR-358 were administered subcutaneously. For each animal, the concentration was adjusted to achieve the specified dose at an injection volume of \approx 5 mL/kg for both agents. NKTR-358 was dosed in protein equivalents, not including the mass of PEG.

2.2. Animals

Animal studies were conducted under accreditation by the Association for Assessment and Accreditation of Laboratory Animal Care, the Canadian Council on Animal Care, or approved by the Institutional Animal Care and Use Committee at PharmaLegacy Laboratories (Pudong, Shanghai, China). All studies met the ethical and humane criteria for transportation, housing, and care established by United States National Institutes of Health guidelines or Canadian animal care regulators.

Female C57BL/6 mice aged 6–8 weeks and weighing 15–20 g were purchased from Charles River Laboratories (Wilmington, MA) or Shanghai SLAC Laboratory Animal Co. Ltd (Shanghai, China). MRL/MpJ-Fas^{lpr} mice were obtained from Shanghai SLAC Laboratory Animal Co. Ltd. Female thymectomized mice were purchased from Charles River Laboratories. All animals were co-housed with dose-group members and provided with a standard irradiated diet and water *ad libitum*.

Young adult male and female cynomolgus monkeys, weighing 2.0–3.3 kg at treatment initiation, were obtained from the Spare Colony at ITR Laboratories Canada Inc. (ITR; Baie d'Urfe, Quebec, Canada) or from Covance Research Products, Inc. (Alice, TX). Animals were co-housed in pairs or groups, except during the initial dosing period. Standard diet and water were available *ad libitum*.

2.3. Flow cytometry immunophenotyping

For flow cytometry of peripheral blood samples (from cynomolgus monkeys, humans, female C57BL/6 mice and spleens from female C57BL/6 mice), fluorescent antibodies against CD3, CD4, CD8, CD25,

FoxP3, Helios, CD39, and Ki67 were obtained from eBioscience (San Diego, CA); against pSTAT5, programmed death-1 (PD-1), CD103, CD73, CD49b, CD134 (OX40), glucocorticoid-induced tumor necrosis factor receptor (GITR), and inducible T-cell co-stimulator (ICOS) from BD Biosciences (San Jose, CA); against CTL-associated antigen-4 (CTLA-4) from Biolegend (San Diego, CA); and against neuropilin-1 from R&D Systems (Minneapolis, MN). Flow cytometry data were acquired using a Fortessa X20 cell analyzer (Becton Dickinson, Franklin Lakes, NJ) and FACSCanto II (Becton Dickinson). Instrument settings (gain, compensation, and threshold) were set with machine software in conjunction with calibration beads, and a total of 100,000 events were collected. Data were analyzed using FlowJo software (FlowJo, LLC, Ashland, OR). After gating on lymphocytes, positive populations were identified based on fluorescence minus one control. Mouse Tregs were defined as CD45⁺CD3⁺CD4⁺CD25⁺FoxP3⁺, cytotoxic T cells as CD45⁺CD3⁺CD8⁺, and NK cells as CD45⁺CD3⁺CD49⁺. All additional markers, Helios, ICOS, GITR, CTLA-4, OX40, Ki67, CD39, CD73, PD-1, CD103, and neuropilin-1, were gated off of the Treg population. Immunophenotyping results were enumerated as percent relative (%) values for each phenotype and mean fluorescence intensity (MFI). Human Tregs were defined as CD3⁺CD4⁺CD25⁺FoxP3⁺, cytotoxic T cells as CD3⁺CD8⁺, and NK cells as CD3⁺CD56⁺.

2.4. IL-2 receptor binding by surface plasmon resonance

Relative binding affinities of rhIL-2 and NKTR-358 for the IL-2R α and IL-2R β receptor subunits were determined using the Biacore X-100 Surface Plasmon Resonance Instrument (GE Healthcare, Chicago, IL). According to the manufacturer's directions, the CM5 chip was activated with a 1:1 mixture of N-hydroxysuccinimide (NHS) 1-ethyl-3-(3-dimethylaminopropyl)-carbodiimide to generate active NHS ester. Goat anti-human Fc antibody (Life Technologies, Carlsbad, CA) was covalently attached to the surface by injecting it for 5 min (\approx 5000 response units) and quenching with 1 M ethanolamine.

At the initiation of each injection cycle, either human IL-2R α -Fc chimera, human IL-2R β -Fc chimera or both, obtained from Symansis (Levels, New Zealand), were captured on the respective sensor chips. Three-fold dilutions of rhIL-2 and NKTR-358 were injected onto the receptor-coated sensor chip. For kinetic measurements, association constant (k_a) rates were measured by flowing analytes for 3 min and dissociation constant (k_d) rates were measured during a 3-min wash step. The ratio between k_d and k_a was used to calculate equilibrium dissociation constant (K_D) values. For steady-state measurements, the response signal from analytes bound during incubation at different concentrations was measured. These signals were plotted against their concentrations, and K_D values were estimated by fitting the curve into an equation governing equilibrium binding.

2.5. *In vitro* STAT5 phosphorylation induction in peripheral blood mononuclear cells and whole blood

Peripheral blood mononuclear cells (PBMCs) from cynomolgus monkeys and human whole blood were obtained from two healthy female and male donors from each species and stimulated *in vitro* with at least 12 different concentrations, \approx 1 log apart, of both NKTR-358 and rhIL-2. NKTR-358 was tested from 0.5×10^{-7} μ g/mL - 150 μ g/mL and rhIL-2 was tested from 0.5×10^{-7} μ g/mL - 100 μ g/mL. Following \approx 45 min of incubation, the induction of phosphorylation of STAT5 was assessed in lymphocytes by flow cytometry. Half maximal effective concentration (EC₅₀) values were calculated from each donor and averaged using the pSTAT5 MFI values. EC₅₀ values for compound dose responses were determined from four-parameter non-linear regression curves using Prism 8. In conjunction with the intracellular pSTAT5 signal, surface markers allowed the comparison of activity between different lymphocyte cell populations.

2.6. Phosphorylation measured by mass cytometry analysis

rhIL-2-induced STAT5 phosphorylation in human PBMCs was also evaluated by mass cytometry [23]. PBMCs isolated from 4 healthy donors were washed with MaxPar Cell Staining Buffer (Fluidigm) and blocked with Human FcR Blocking Reagent (Miltenyi Biotec, Bergisch Gladbach, Germany) for 10 min at room temperature. Cells were then incubated with a panel of metal-conjugated antibodies targeting cell surface markers (S1 Table) for 30 min at room temperature and then washed twice with cell staining buffer. After washing, cells were incubated in pre-warmed phosphate-buffered saline supplemented with 2% fetal bovine serum (FBS) for 15 min at 37 °C with 5% CO₂, and then stimulated with different concentrations of NKTR-358 or rhIL-2 (0.003 μ g/mL - 30 μ g/mL) for 15 min at 37 °C. To halt signal transduction after stimulation, cells were immediately fixed with Cytofix™ Fixation Buffer (BD Biosciences) and permeabilized with Phosflow™ Perm Buffer III (BD Biosciences) according to manufacturer's instructions. Fixed/permeabilized cells were washed twice with cell staining buffer and incubated with a panel of metal-conjugated antibodies targeting intracellular antigens for 30 min at room temperature. After staining with intracellular antibodies, cells were washed twice with cell staining buffer and incubated with 191/193Ir DNA intercalator (Fluidigm) according to manufacturer's instructions. Prior to mass cytometry analysis, cells were washed twice with cell staining buffer and twice with MaxPar Water (Fluidigm).

Cells were analyzed on a CyTOF® 2 mass cytometer (Fluidigm) at an event rate of \approx 500 cells/second. To normalize CyTOF data over different days, EQTM Four Element Calibration Beads (Fluidigm) were added in all samples. Resulting data were analyzed with software available through Cytobank (www.cytobank.org). To remove debris and doublets, single cells were gated based on cell length and DNA content as described by Bendall et al. [24]. To interpret high-dimensional single-cell data that were produced by mass cytometry, we used a visualization tool based on the t-Distributed Stochastic Neighbor Embedding algorithm (t-SNE), which allows visualization of high-dimensional cytometry data on a two-dimensional map at single-cell resolution and preserves the nonlinearity [25]. The t-SNE plots were all normalized to the same scale (0–200).

2.7. Pharmacodynamic evaluation of Treg mobilization, activation, and proliferation in mice

Female C57BL/6 mice (n = 32 animals per dose group) were administered a single subcutaneous dose of either vehicle control (10 mM sodium acetate, 200 mM sodium chloride, 2% sucrose, pH 5, prepared in sterile water for injection) or NKTR-358 (0.03, 0.1, or 0.3 mg/kg per dose). In a separate study, female C57BL/6 mice (n = 45 animals per dose group) were administered five consecutive, once-daily, subcutaneous doses of rhIL-2 (0.1, 0.3 or 1 mg/kg) or vehicle control (rhIL-2 formulation buffer). Peripheral blood was collected via cardiac puncture and pooled at 1, 2, 3, 4, 5, 6, 7, and 10 days after the initial dose of NKTR-358 or rhIL-2. Animals treated with rhIL-2 or control also had blood samples collected at 14 days. In thymectomized mice, vehicle control or NKTR-358 (0.1 mg/kg) was administered as a single subcutaneous dose, and peripheral blood samples were collected at 2, 4, 5, 7, and 10 days after dosing. In an additional study to evaluate peripheral Treg (pTreg)- and natural Treg (nTreg)-derived cells, female C57BL/6 mice received a single subcutaneous dose of vehicle or NKTR-358 (0.3 mg/kg) and peripheral blood samples were collected 4 days after dosing for neuropilin-1 expression. Blood samples were analyzed by immunophenotyping and flow cytometry, as described above.

2.8. *Ex vivo* murine T-cell suppression assay

Spleens were collected from female C57BL/6 mice treated with NKTR-358 at 0.03, 0.1, and 0.3 mg/kg or vehicle at 1, 2, 3, 4, 5, 6, 7, and

10 days after dose administration ($n = 4$ mice/treatment group/time point). Single-cell splenocyte suspensions were prepared and pooled for each dose group at each timepoint.

CD4⁺CD25⁺ Tregs were isolated from spleen preparations by magnetic-activated cell sorting using the mouse CD4⁺CD25⁺ Regulatory T Cell Isolation Kit (Miltenyi Biotec) according to the manufacturer's recommendations. CD4⁺ T cells were negatively selected and then separated into CD4⁺CD25⁻ T cells and CD4⁺CD25⁺ Tregs. Naïve CD4⁺CD25⁻ Tcons were isolated from mouse spleens harvested from untreated animals, using the naïve CD4⁺ T Cell Isolation Kit (Miltenyi Biotec) and following the manufacturer's recommended procedure.

In vitro suppression assays were carried out in RPMI 1640 medium supplemented with 10% FBS, 2 mM L-glutamine, 1 mM sodium pyruvate, 0.5 μ M β -mercaptoethanol, 100 units/mL penicillin, 100 μ g/mL streptomycin, and 250 ng/mL amphotericin B. Tcons (5×10^4) were stimulated with beads coated with anti-CD3 and anti-CD28 (mouse T Cell Activation/Expansion Kit, Miltenyi Biotec) at a ratio of two beads per Tcon in 96-well round-bottom plates. The suppressive capacity of Tregs was assessed by the addition of Tregs to Tcons at different ratios (Treg:Tcon ratios of 2:1 to 1:512). Each Treg:Tcon ratio was tested in triplicate. Cells were co-cultured for 72 h at 37 °C and 5% CO₂ in a humidified atmosphere; 16 h prior to the termination of the assay, 0.5 μ Ci [³H]-thymidine was added to wells. After washing cells to remove unincorporated [³H]-thymidine, thymidine uptake was measured as counts per minute (CPM) using a microplate scintillation counter (TopCount NXT, PerkinElmer). Individual CPM values were normalized to maximal proliferation.

2.9. Pharmacokinetic evaluation of NKTR-358 in mice (single dose) and cynomolgus monkeys (single and repeat doses)

Doses were calculated based on protein equivalents for all *in vivo* studies. Female C57BL/6 mice received a single subcutaneous dose of NKTR-358 (0.03, 0.1, and 0.3 mg/kg). Blood samples (\approx 500 μ L) were collected and combined from each mouse ($n = 4$ /time point) at 1, 2, 4, and 8 h and 1, 2, 3, 4, 5, 6, 7, and 10 days post dose.

For single-dose NKTR-358 PK assessment, cynomolgus monkeys (one male and one female per dose group) received either a single subcutaneous or intravenous dose of NKTR-358 (25 μ g/kg) or five sequential, daily subcutaneous doses of rhIL-2 (5 μ g/kg/day). Injection volumes were kept constant at 0.2 mL/kg regardless of route and test article. Blood samples (\approx 0.3 mL on day 1 and 0.5 mL all other occasions) were collected by venipuncture into vacutainer-containing K₂EDTA as anticoagulant from each monkey. Time points for NKTR-358 were day -1; 2 min, 5 min, 15 min, 30 min, 1 h, 4 h, 8 h, and 12 h post dose; and at 24, 48, 72, 96, 120, 144, 168, 336, and 504 h post dose (\pm 2 h). For rhIL-2, blood samples were taken at the following time points: day -1; 2 min, 5 min, 15 min, 30 min, 1 h, 4 h, and 8 h post dose on days 1 and 5. For repeat-dose NKTR-358 PK evaluation, cynomolgus monkeys (3-7/sex/group) received a subcutaneous dose of NKTR-358 at 0 (vehicle control), 30, 90, or 150 μ g/kg once every other week (biweekly) for 6 months. Injection volumes were 0.6 mL/kg. Blood samples (\approx 0.5 mL on days 1, 99 [dose 8] and 155 [dose 13]) were collected by venipuncture from each monkey. Time points were day -1 and at 2, 4, 12, 24, 48, 72, 96, 144, 216, and 336 h post dose.

Following blood collection, the samples from all PK studies were centrifuged (2500 rpm for 5 min at \approx 4 °C) and the resulting plasma was recovered and stored frozen (\leq -60 °C) until analysis by a qualified Ligand Binding Assay (LBA). PK parameters were determined by non-compartmental analysis using Phoenix® WinNonlin® (Version 6.4; Certara USA, Inc., Princeton, NJ).

2.10. Bioanalytical method for NKTR-358 determination

The plasma concentrations of NKTR-358 were quantified by an indirect LBA. A rabbit monoclonal antibody to methoxy PEG (Abcam) was

used as a coating antibody bound to Meso Scale Discovery (MSD) high-bind plates. NKTR-358 was used to generate the Calibration Standards (CS) and assay Quality Control samples (QCs) by serial dilution in the control matrix. A combination of two biotinylated, mouse monoclonal antibodies to human IL-2 (Mabtech and R&D Systems) were used as detecting antibodies. Ruthium (II) tris-pyridine conjugated streptavidin (SAV Sulfo-TAG, MSD) was used for signal. After the addition of read buffer (MSD), the sample plates were read on an MSD Sector Imager 2400 and data analysis was performed using Discovery Workbench software. The calibration curves (CCs) were obtained using a weighted (1/y²), four-parameter regression to fit the plot of the mean electrochemiluminescence at each CS level versus nominal concentration. The CSs, QCs, and sample concentrations were calculated by interpolation with the CCs. The lower limit of quantification was 0.1 ng/mL.

2.11. Biomarker evaluation of NKTR-358 in cynomolgus monkeys

For hematology from the single-dose NKTR-358 and repeat rhIL-2 PK study, blood samples (nominal 0.5 mL) were collected by venipuncture into K₂EDTA anticoagulant tubes for the measurement of serum IL-5 and eosinophils. Serum that was separated from collected blood samples pre-dose (relative to the first dose of IL-2 and single dose of NKTR-358) and on days 2, 3, 4, 5, 6, 7, 14 and 21 post dosing were analyzed for IL-5 using the LEGENDplex™ (BioLegend, San Diego, CA) non-human primate kit according to the vendor's instructions. Fluorescence intensity was quantified on a flow cytometer (BD FACS Canto™ II) and data were analyzed using LegendPlex™ Data Software. Eosinophils were analyzed from samples collected at day 14 post dosing using the Advia120, Hematology Analyzer.

For immunophenotyping in the NKTR-358 repeat-dose study, \approx 1 mL of blood was collected from each animal by venipuncture into tubes containing the anticoagulant K₂EDTA. Samples were collected twice pre-treatment and on days 1, 3, 8, 15, 99, 101, 106, 113, 169, 171, 176, and 183. Tubes were placed in ice until analyses of Treg populations by flow cytometry.

2.12. Effect of NKTR-358 on the development and progression of the MRL/MpJ-Fas^{lpr} mouse model of systemic lupus erythematosus

Forty-five 5- to 7-week-old MRL/MpJ-Fas^{lpr} mice were randomized after at least 1 week of acclimatization into three test groups ($n = 15$ per dose group) based on body weight and level of protein content in urine. At week 8, animals were treated with vehicle or NKTR-358 at 0.03 or 0.3 mg/kg, twice weekly for 12 weeks. A fourth disease-free mouse strain control group, consisting of C57BL/6 mice ($n = 3$), received vehicle alone on the same dosing schedule to serve as a negative control. Mice were monitored daily for their health condition. Body weight was measured twice weekly. Urine samples were collected on plastic wrap with gentle bladder massage at baseline (1 day immediately prior to dosing) and weekly thereafter. Protein level in the urine was measured on a Siemens Clinitek Status Analyzer. Three mice from each test group were humanely sacrificed 3 days after the first dose administration (study week 8), and all remaining mice were humanely sacrificed 3 days after the final dose (study week 20). Blood samples were collected and aliquoted for serum preparation and clinical biochemistry (centrifuged at 10,000 rpm for 10 min and stored at -80 °C) or for flow cytometry (collected in EDTA-K tubes). At the end of week 20, kidneys were collected for histological evaluation. Kidney slides from a transverse section from the right kidney and a longitudinal (sagittal) section from the left kidney were prepared, stained, and scored by a pathologist. Scoring methodology is provided in S2 Table.

For clinical biochemistry, serum was analyzed for anti-double-stranded DNA (dsDNA) antibodies by ELISA (mouse anti-dsDNA IgG-specific ELISA kit, Alpha Diagnostic International, San Antonio, TX) and for blood urea nitrogen (BUN) concentration using a HITACHI 7020 Automatic Biochemistry Analyzer. EDTA-whole blood was analyzed for

lymphocyte populations by flow cytometry.

2.13. Statistical analysis

For flow cytometry immunophenotyping, Prism 8 (GraphPad Software, San Diego, CA) was used to calculate area under the curve (AUC) and fold changes and to conduct statistical analyses using unpaired t-tests.

For the *in vitro* suppression assays, statistical analyses were

performed using unpaired, 2-tailed t-tests in Prism 8 (GraphPad Software, San Diego, CA) to compare differences between treated and control groups at individual Treg:Tcon ratios and at specific times post-dose.

2.14. Ethics approval and consent to participate

Animal studies were performed under protocols approved by the Institutional Animal Care and Use Committee of Nektar Therapeutics and the Canadian Council on Animal Care. All studies met the ethical

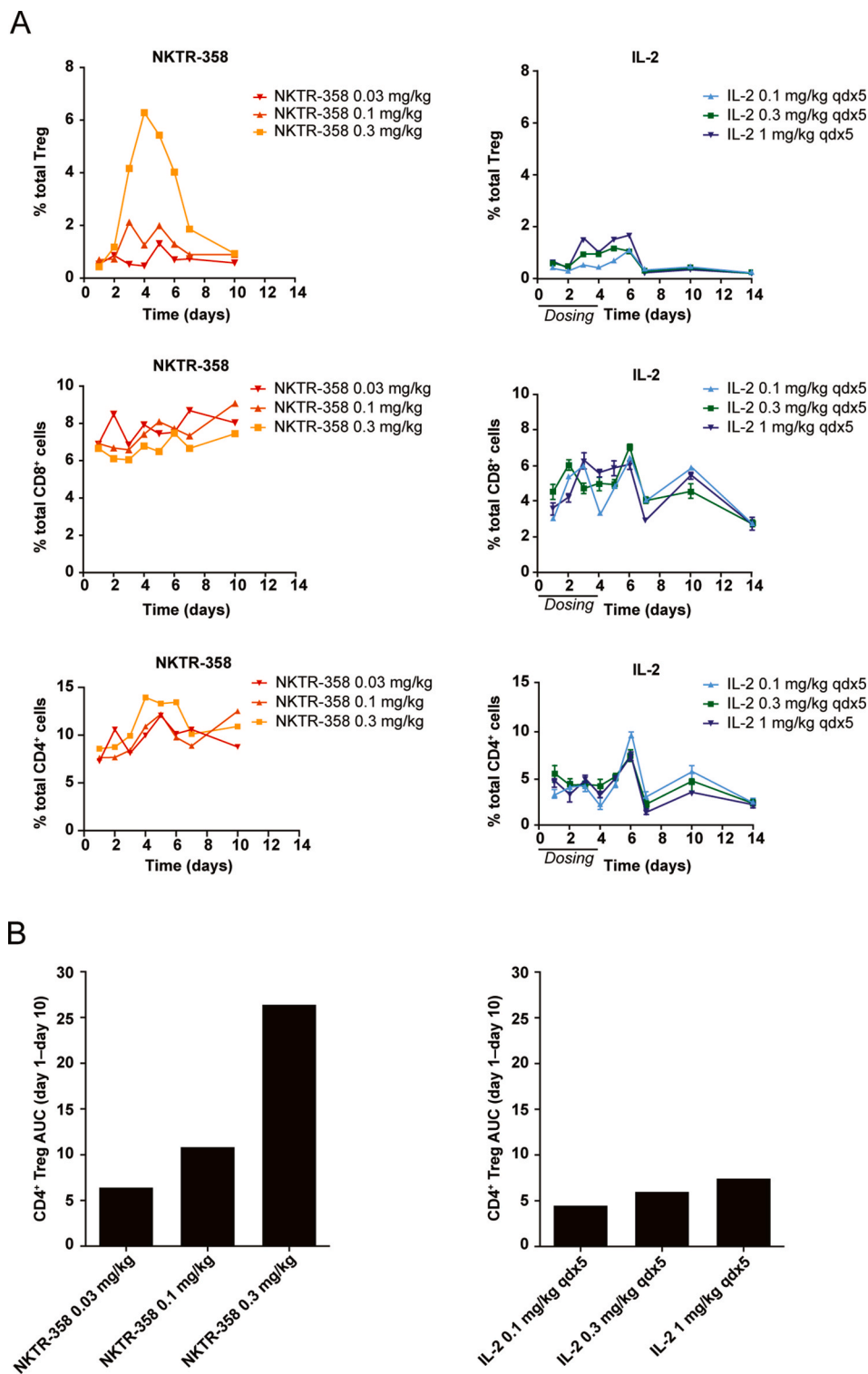


Fig. 1. A single subcutaneous dose of NKTR-358 is sufficient to promote Treg mobilization in blood. Female C57BL/6 mice were administered either a single subcutaneous dose of vehicle control, NKTR-358 (0.03, 0.1, or 0.3 mg/kg); or 5 consecutive, once-daily, subcutaneous doses of IL-2 (0.1, 0.3, or 1 mg/kg). **(A)** Blood was analyzed for the presence of Treg (CD4⁺CD25⁺Foxp3⁺), CD8⁺ and CD4⁺ T cells after gating on lymphocytes. NKTR-358-treated mice samples were pooled (n = 4) prior to flow analysis as compared with IL-2-treated mice (n = 5). **(B)** To quantify the changes in Treg over time, the AUC was determined for each condition in A. AUC, area under the curve; qd, once daily; Treg, regulatory T cell.

and humane criteria for transportation, housing, and care established by United States NIH guidelines or Canadian animal care regulators.

3. Results

3.1. A single administration of NKTR-358 in mice promotes greater Treg expansion compared with multiple IL-2 administrations

We identified NKTR-358 through an *in vivo* screening of 23 PEG IL-2 conjugates. Unlike *in vitro* screening, an *in vivo* screening funnel enables the aggregate biochemical and pharmacological properties of the potential drug candidate to be evaluated. NKTR-358, was ultimately selected for its unique ability to robustly increase Treg numbers with limited effect on other CD4⁺ and CD8⁺ T-cell populations. Induction of Treg expansion was compared between a single subcutaneous administration of NKTR-358 (0.03, 0.1, or 0.3 mg/kg) and five consecutive daily subcutaneous doses of 0.1, 0.3, or 1 mg/kg rhIL-2 (total dose of 0.5, 1.5, or 5 mg/kg) in female C57BL/6 mice. Flow cytometric immunophenotyping demonstrated that a single 0.3 mg/kg subcutaneous administration of NKTR-358 promoted more than a 20-fold change in Treg mobilization in the peripheral blood, as compared with only a 5-fold change after multiple doses of rhIL-2 at 1 mg/kg (Fig. 1A). Hence, a single NKTR-358 injection at an approximate 17-fold lower dose than that of rhIL-2 elicited a 4-fold higher Treg production. The maximum dose of rhIL-2 resulted in the same level of Treg fold-change as a dose of NKTR-358 that was 50-times lower (Fig. 1A). The 0.03-mg/kg dose of NKTR-358 had a minimal effect on mobilizing Tregs. By day 10, the percent of Tregs in peripheral blood of all NKTR-358-treated animals had returned to levels observed in control animals. NKTR-358 had a minimal effect on CD8⁺ and total CD4⁺ T cells, exhibiting less than a 2-fold change in these populations at the highest concentration (Fig. 1A). Similar results were observed for CD4⁺ CD25⁻ cells, which also exhibited less than a 2-fold change (data not shown).

The area under the Treg effect curve (Treg AUC) was calculated to compare the effective difference of Treg induction between NKTR-358 and rhIL-2. These Treg AUC values, calculated between day 1 and day 10, were greater for NKTR-358 compared with rhIL-2 (Fig. 1B). While AUC values from single versus multi-dose may not be directly comparable, a single 0.1-mg/kg and 0.3-mg/kg dose of NKTR-358 resulted in 2- to 5-fold larger AUC than that of multiple doses of rhIL-2 at 0.1, 0.3 and 1 mg/kg. Thus, rhIL-2 dosed maximally for 5 days is unable to achieve the magnitude of Treg mobilization observed with a single 0.1-mg/kg or 0.3-mg/kg dose of NKTR-358. In addition, assessment of the PK profile of subcutaneous administration of NKTR-358 in mice showed that its elimination half-life of 1.9–2.2 days (data not shown) was substantially longer than that of rhIL-2 (~13 min) from literature data [26], consistent with the observed exposure for NKTR-358. Overall, these data together demonstrate NKTR-358's enhanced specificity towards Treg induction and improved PK in comparison with rhIL-2.

Table 1
NKTR-358 demonstrates attenuated affinity for IL-2Rβ compared with rhIL-2. Human IL-2Rα-Fc chimera, IL-2Rβ-Fc chimera, or both were captured on a Biacore surface plasmon resonance sensor chip and challenged with 3-fold dilutions of IL-2 and NKTR-358. Binding affinities to the IL-2Rα and IL-2Rβ subunits and the heterodimeric IL-2Rαβ were determined by surface plasmon resonance using both kinetic and steady-state measurements [22]. The K_D values from both methods were in close agreement, and therefore, analysis was based on average K_D values from both measurements. The ratio between k_d and k_a were used to calculate the K_D values. Table shows ratios of K_D values. k_a, association rate constant; k_d, dissociation rate constant; KD, equilibrium dissociation constant.

Receptor	rhIL-2 (K _D , nM)	NKTR-358 (K _D , nM)	Ratio NKTR-358/rhIL-2
α	4.3	7300	1700
β	530	88,000	170
αβ	0.071	1700	24,000

Table 2
NKTR-358 favors activation of Treg over Tcon as compared with IL-2. PBMCs from cynomolgus monkey and human whole blood were obtained from two healthy female and male donors from each species and stimulated *in vitro* with at least 12 different concentrations ≈1 log apart of each test item. pSTAT5 MFI on different lymphocyte populations was measured by flow cytometry and used to determine EC₅₀ values. An EC₅₀ was calculated from each donor for each population and averaged. EC₅₀, half maximal effective concentration; MFI, mean fluorescence intensity; PBMC, peripheral blood mononuclear cell; SD, standard deviation; Tcon, conventional T cell; Treg, regulatory T cell.

Test material	pSTAT5 EC ₅₀ (mean ± SD), ng/mL		CD3 ⁺ T cells		CD4 ⁺ CD25 ⁺ T cells		CD8 ⁺ T cells		CD4 ⁺ CD25 ⁺ CD8 ⁺ ratio	
	Monkey PBMCs	Human PBMCs	Monkey PBMCs	Human PBMCs	Monkey PBMCs	Human PBMCs	Monkey PBMCs	Human PBMCs	Monkey PBMCs	Human PBMCs
rhIL-2	8.87 ± 4.77	1.34 ± 0.416	0.0166 ± 0.00924	0.0198 ± 0.00357	12.7 ± 7.36	6.22 ± 2.041	0.001 ± 0.001	0.003 ± 0.001	0.001 ± 0.001	0.003 ± 0.001
NKTR-358	4760 ± 2480	4020 ± 1410	50.5 ± 21.6	148 ± 58.3	5450 ± 2786	4720 ± 2121	0.01 ± 0.002	0.034 ± 0.017	0.01 ± 0.002	0.034 ± 0.017
Ratio NKTR-358/rhIL-2	550 ± 100	3083 ± 1065	4655 ± 4354	7229 ± 1985.8	441 ± 87.9	757 ± 204.9	-	-	-	-

3.2. NKTR-358 demonstrates attenuated binding affinity for IL-2 receptor subunits

Following selection of NKTR-358 from the *in vivo* screening cascade, we next aimed to investigate the relative affinities of NKTR-358 and rhIL-2 for the IL-2 receptor complex *in vitro* to characterize the receptor-binding dynamics that could underly the selectivity we observed in the Treg/Tcon response. Overall, NKTR-358 had significantly decreased affinities for all IL-2 receptor components and complexes compared with rhIL-2.

The binding affinities to IL-2R α , IL-2R β , and IL2R $\alpha\beta$ for rhIL-2 and NKTR-358 are summarized in Table 1. For IL-2R α and IL-2R β , NKTR-358 had slower on-rates and similar off-rates compared with rhIL-2, resulting in 1700-fold and 170-fold lower affinities for the respective receptor subunits. For the heterodimeric IL-2R $\alpha\beta$, NKTR-358's affinity was more than 24,000-fold lower than rhIL-2, due to NKTR-358's much slower on-rate, while the difference in off-rates was only \approx 2-fold. Taken together, these data demonstrate that the unique structure of NKTR-358 bestows it with a shifted affinity profile that has much lower binding affinity to all IL-2 receptors compared with rhIL-2.

3.3. NKTR-358 favors induction of phosphorylated STAT5 in Tregs over Tcons

We next assessed STAT5 phosphorylation in human and cynomolgus monkey PBMCs *in vitro* after NKTR-358 or rhIL-2 treatment. PBMCs consist of a mixture of cell populations including Tregs and Tcons and thus allow the simultaneous assessment of cell signaling potency as well as cell enumeration using flow cytometry. NKTR-358 induced pSTAT5 activity in CD3⁺, CD4⁺CD25⁺ and CD8⁺ T cells (Table 2 and S1A Fig) and showed a similar pattern of cell type sensitivity across both species. CD4⁺CD25⁺ T cells (the population most enriched for Tregs) displayed the greatest sensitivity to NKTR-358 in comparison with total CD3⁺ and CD8⁺ T cells. The higher CD4⁺CD25⁺/CD8⁺ pSTAT5 EC₅₀ ratio

observed with NKTR-358 in both monkey and human PBMCs demonstrates the compound's preferential selectivity for Tregs over CD8⁺ T cells. In all T-cell subtypes, and regardless of species, NKTR-358 exhibited much lower potency relative to rhIL-2. This finding agrees with the data from biochemical binding studies, which demonstrate that NKTR-358 displays attenuated IL-2 receptor engagement.

We further examined the pSTAT5 response to NKTR-358 in human PBMCs using CyTOF technology. Consistent with the flow cytometry data above, the effect was primarily limited to Tregs, including Helios⁺ and Helios⁻ naive and memory Tregs with minimal effect on Tcons, NK or CD8 T cells (Fig. 2 and S1C Fig). As expected from the difference in potency, rhIL-2 induced pSTAT5 in all Tregs and non-Treg populations at lower doses. (S1B and S1C Figs). No measurable activity was observed for pAKT, pERK, or pS6 with rhIL-2 or NKTR-358.

3.4. NKTR-358 leads to dose-dependent increases in Treg functional markers

Taken together, our *in vitro* findings support NKTR-358's preferential activation of Tregs over Tcons compared with rhIL-2, and we also demonstrated that NKTR-358 induced a dose dependent increase in Tregs in mice (Fig. 1A). We next investigated changes in non-Treg cell populations as well as Treg functional markers upon treatment with NKTR-358 in the mouse model. NKTR-358 treatment led to no changes in CD8⁺ T cells and a minimal \approx 2-fold peak increase in NK cells at the 0.3-mg/kg dose (Fig. 3A). Treg levels of CD25 and FoxP3, established markers of Tregs [27,28] and their immunosuppressive function [29, 30], increased in a dose-dependent manner. In animals administered the 0.3-mg/kg NKTR-358 dose, peak MFI of CD25 and FoxP3 occurred on day 2, with a 4-fold increase in CD25 and an \approx 2-fold increase in FoxP3 MFI, relative to control animals (Fig. 3A).

NKTR-358 also induced Treg proliferation *in vivo*; the proportion of proliferative (Ki67⁺) Tregs increased between days 2 and 7 after administration of 0.1 and 0.3 mg/kg NKTR-358. In animals dosed with

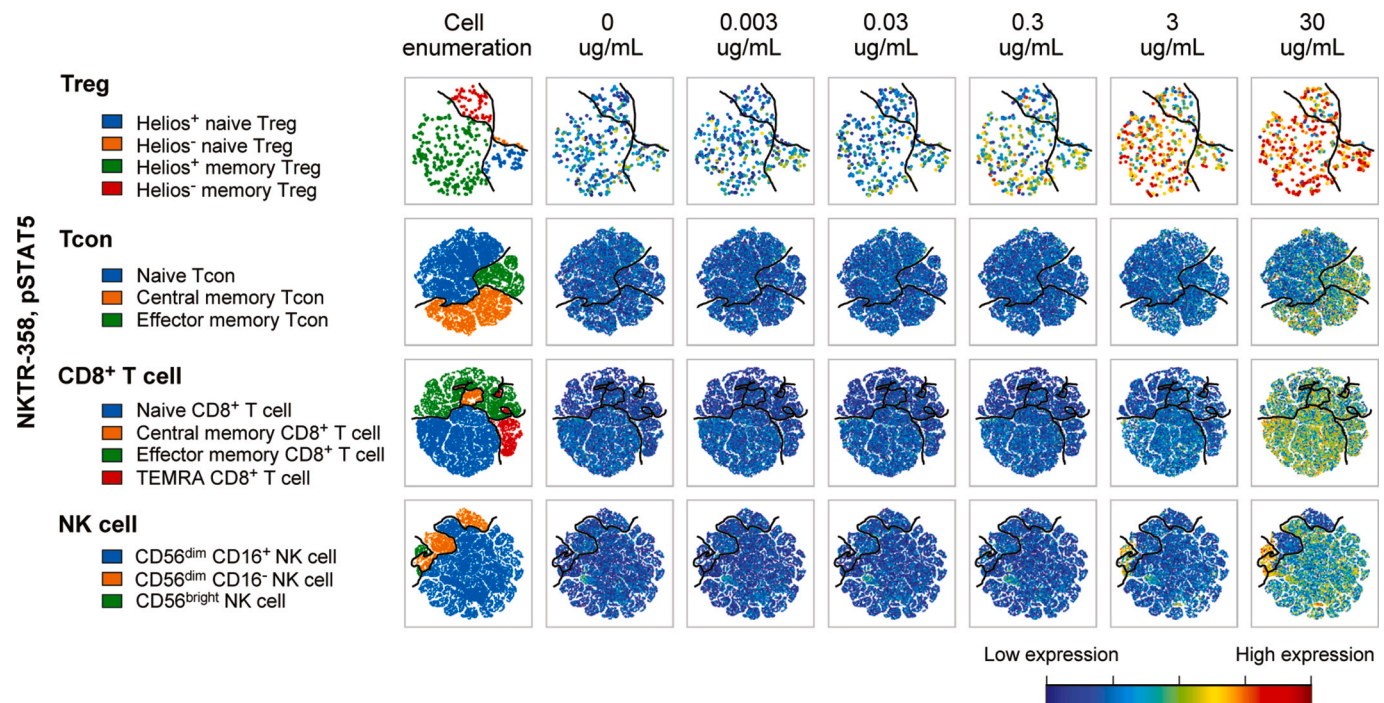


Fig. 2. NKTR-358 favors activation of Treg over Tcon. PBMCs from 4 healthy donors were incubated with varying concentrations of NKTR-358 for 15 min. PBMCs were stained with a panel of 35 metal-conjugated antibodies and analyzed by CyTOF. viSNE plots were used to visualize expression of each marker in individual cells. Plots shown here demonstrate expression of pSTAT5 in various phenotypically defined subsets of Treg, CD4⁺, CD8⁺ T cells and NK cells. Expression of pSTAT5 is normalized for all plots in cells from a single healthy donor with red color indicating high expression and dark blue indicating lack of expression. NK, natural killer; PBMC, peripheral blood mononuclear cell; Tcon, conventional T cell; Treg, regulatory T cell.

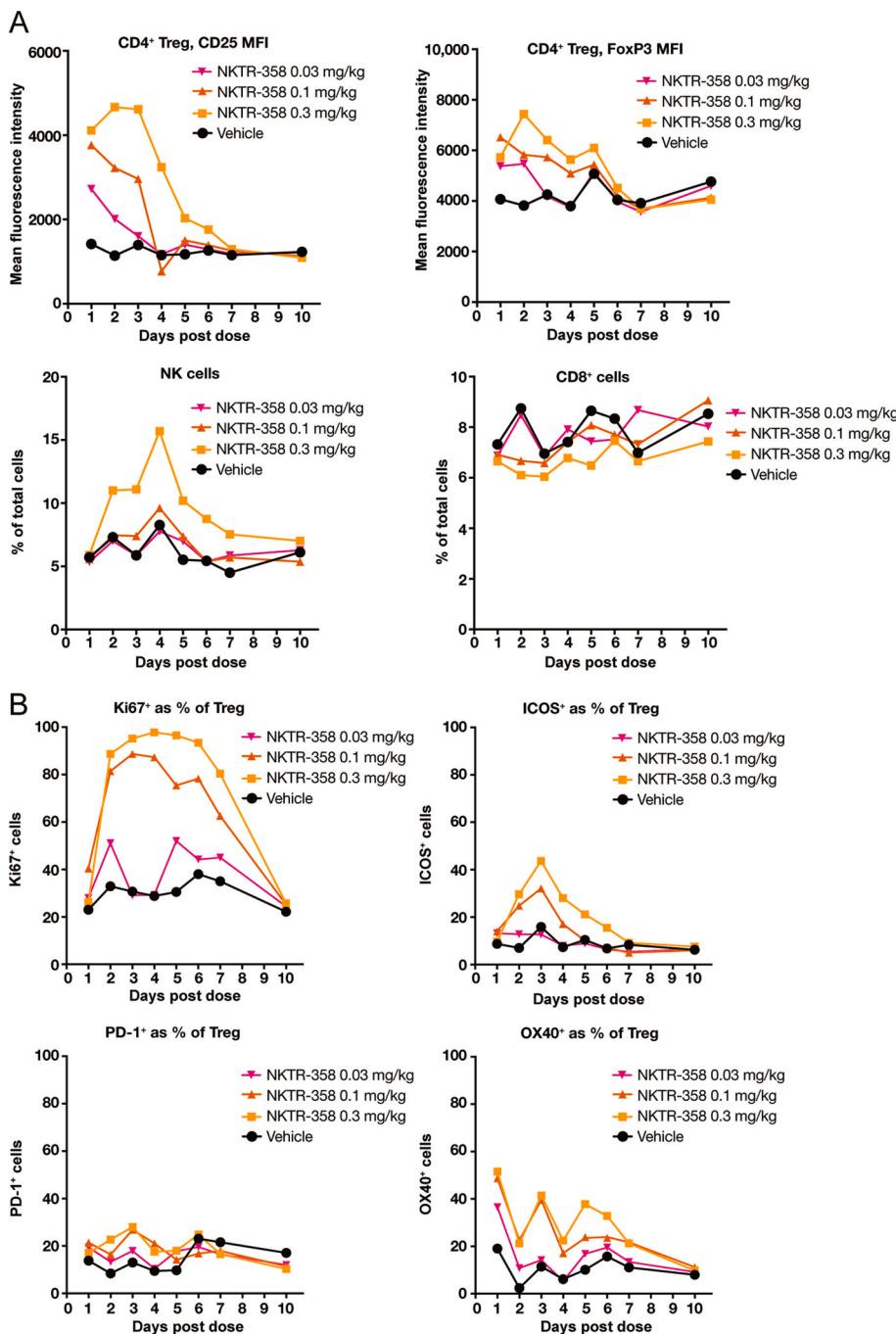


Fig. 3. NKTR-358 promotes proliferation and activation of Treg with minimal stimulation of CD8⁺ T cells and NK cells. Female C57BL/6 mice were administered either a single subcutaneous dose of vehicle control or NKTR-358 (0.03, 0.1, or 0.3 mg/kg). (A) and (B) Blood samples were analyzed for markers of CD8⁺ T cells, NK cells, and Treg proliferation and activation after gating on lymphocytes. ICOS, inducible T-cell co-stimulator; MFI, mean fluorescence intensity; NK, natural killer cell; PD-1, programmed death-1; Treg, regulatory T cell.

0.3 mg/kg NKTR-358, over 80% of Tregs were positive for Ki67 during days 2–7 compared with less than 40% in control animals (Fig. 3B and S2 Fig). Both the 0.1-mg/kg and 0.3-mg/kg dose levels maintained a greater than 2-fold increase in the Ki67⁺ Treg population from day 2 to day 6. The proportion of proliferative cells within the peripheral Treg population returned to levels of the control group by day 10.

Administration of NKTR-358 also resulted in an increase in the percentage of Tregs that expressed ICOS, which plays an important role in the suppressive function mediated by Tregs [31,32]. The percentages of ICOS⁺ Tregs in animals treated with 0.1 and 0.3 mg/kg doses were greater than those of the control animals from day 2 to day 4 with a peak at day 3 (Fig. 3B and S2 Fig). An ≈3-fold increase in ICOS⁺ Tregs was observed at days 2 and 3 in animals administered the 0.3-mg/kg dose relative to control animals. Induction of additional key Treg activation markers such as PD-1 and OX40 by NKTR-358 was also noted [33–36].

The 0.3-mg/kg dose of NKTR-358 induced a greater than 2-fold increase in PD-1⁺ Tregs and a greater than 9-fold increase in OX40⁺ Tregs at day 2 when compared with vehicle (Fig. 3B and S2 Fig). In addition, in animals receiving the 0.3 mg/kg dose, CTLA-4 MFI increased by 2-fold between day 2 and day 4 and GITR MFI was greater than 3-fold higher as compared with control animals (data not shown). Other functional markers were evaluated such as CD39, CD103 and CD73, but changes in their levels were of minimal magnitude (data not shown).

3.5. NKTR-358 induces natural, thymic-derived Tregs and peripherally derived Tregs in mouse peripheral blood

We investigated whether the NKTR-358-induced CD4⁺ Tregs observed in our studies were thymic-derived, nTreg-like cells or were naïve CD4⁺ T cells that had been induced to differentiate outside the

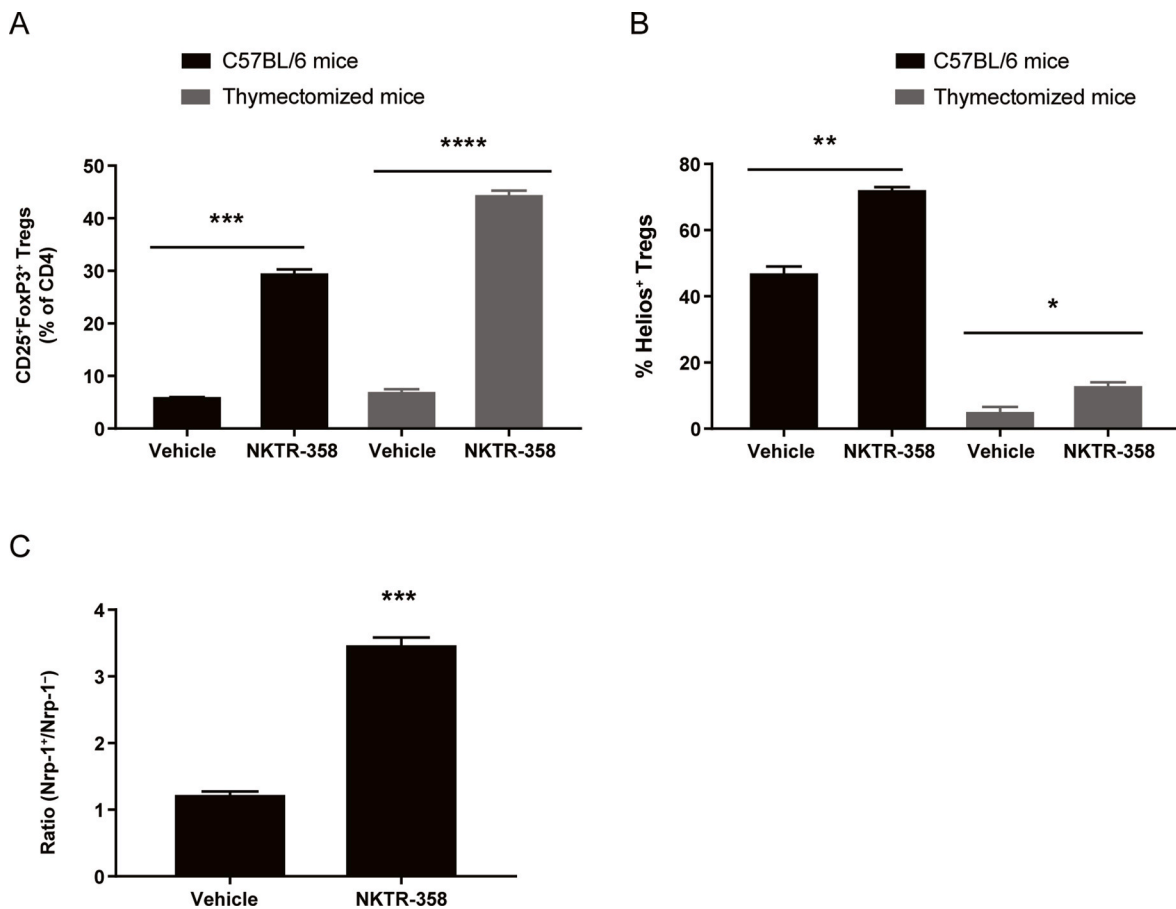


Fig. 4. NKTR-358 induces both natural and peripheral Treg populations. (A) and (B) Female C57BL/6 mice and thymectomized mice were administered either a single subcutaneous dose of vehicle control or NKTR-358 (0.1 mg/kg). Blood samples were analyzed for Tregs and markers of thymic Treg origin (Helios⁺) after gating on lymphocytes. (C) Female C57BL/6 mice received a single subcutaneous dose of vehicle or NKTR-358 (0.3 mg/kg) and peripheral blood was collected 4 days after dosing. Blood samples were analyzed for neuropilin-1⁺ and neuropilin-1⁻ cells by flow cytometry after gating on lymphocytes. Statistical analyses were conducted with unpaired t-tests. *p < 0.05; **p < 0.01; ***p < 0.001; ****p < 0.0001. Nrp-1, neuropilin-1; Treg, regulatory T cell.

thymus (pTreg-like cells). NKTR-358 induced a similar increase in total Tregs (CD25⁺FoxP3⁺) in normal C57BL/6 and thymectomized C57BL/6 mice (~30% and 44%, respectively; Fig. 4A). This induction of Tregs in normal and thymectomized mice was significant when compared with vehicle-treated animals (p = 0.0002 and p < 0.0001, respectively). However, when comparing the origin of these Tregs, NKTR-358 largely induced Tregs expressing Helios (72%), a marker reported to be expressed by thymic-derived Tregs (nTreg-like), in normal C57BL/6 mice, whereas a substantially reduced proportion of Helios⁺ Tregs (13%) was observed in thymectomized mice. Helios⁺ Tregs in both normal C57BL/6 mice and in thymectomized mice were significantly induced when compared with untreated vehicle (p = 0.002 and p = 0.03, respectively). These data suggest that NKTR-358 primarily induces Helios⁺ Tregs but can also induce pTregs that have differentiated outside the thymus (Fig. 4B). Additional studies (data not shown) demonstrated that normal mice that received a single dose of NKTR-358 at 0.1 mg/kg and 0.3 mg/kg exhibited elevated levels of Helios⁺ Tregs from day 1 to day 6 when compared with control animals. Animals treated with 0.1 mg/kg NKTR-358 demonstrated an approximate 70% induction in Helios⁺ Tregs as compared with ~45% induction in vehicle-treated mice.

Since there is much debate on the use of Helios as a comprehensive marker for thymic origin Tregs [26], we also assessed neuropilin-1 expression to further evaluate the balance between natural and peripheral Tregs after NKTR-358 administration. A high level of neuropilin-1 is known to be expressed on naturally derived Treg cells and can be used to separate nTreg-like cells versus pTreg-like cells.

NKTR-358 significantly increased the nTreg:pTreg ratio when compared with vehicle-treated animals (p = 0.0001). NKTR-358 induced 75% neuropilin-1⁺ Tregs and 22% neuropilin-1⁻ Tregs, a 3:1 ratio, whereas vehicle-treated animals exhibited 55% neuropilin-1⁺ Tregs and 43% neuropilin-1⁻ Tregs, a 1:1 ratio (Fig. 4C). Overall, these data suggest that NKTR-358 can expand both thymic- and peripherally derived Treg populations.

3.6. NKTR-358 enhances Treg suppressive capacity

We next investigated whether NKTR-358 would modulate Treg effector function using an *ex vivo* proliferation/suppression assay. Splenic Tregs isolated from mice treated subcutaneously with NKTR-358 or vehicle were co-cultured *in vitro* with Tcons across a range of Treg:Tcon ratios. Tregs isolated from mice on day 1 following NKTR-358 dosing were able to suppress Tcon proliferation up to 92.6% (7.4% ± 1.2% maximal Tcon proliferation) at a Treg:Tcon ratio of 1:2, and considerable suppressive effects (52.3%; 47.7% ± 8.6% maximal Tcon proliferation) were observed even at a 1:16 ratio (Fig. 5A). In contrast, Tregs from vehicle-treated mice suppressed proliferation by only 60.8% (39.2% ± 18.7% proliferating Tcons) at a Treg:Tcon ratio of 1:2 and lost their suppressive capacity (31.5%; 68.5% ± 5.2% maximal Tcon proliferation) at a 1:8 ratio. Suppression levels were significantly higher with NKTR-358-treated Tregs vs vehicle-treated Tregs, with differences between the two groups noted at Treg:Tcon ratios of 1:2, 1:8, and 1:16 (p < 0.05, with a 2-tailed unpaired t-test) for Tregs isolated one day after dosing, and at Treg:Tcon ratios of 1:2, 1:4, 1:8, 1:16, and 1:32 (p < 0.05,

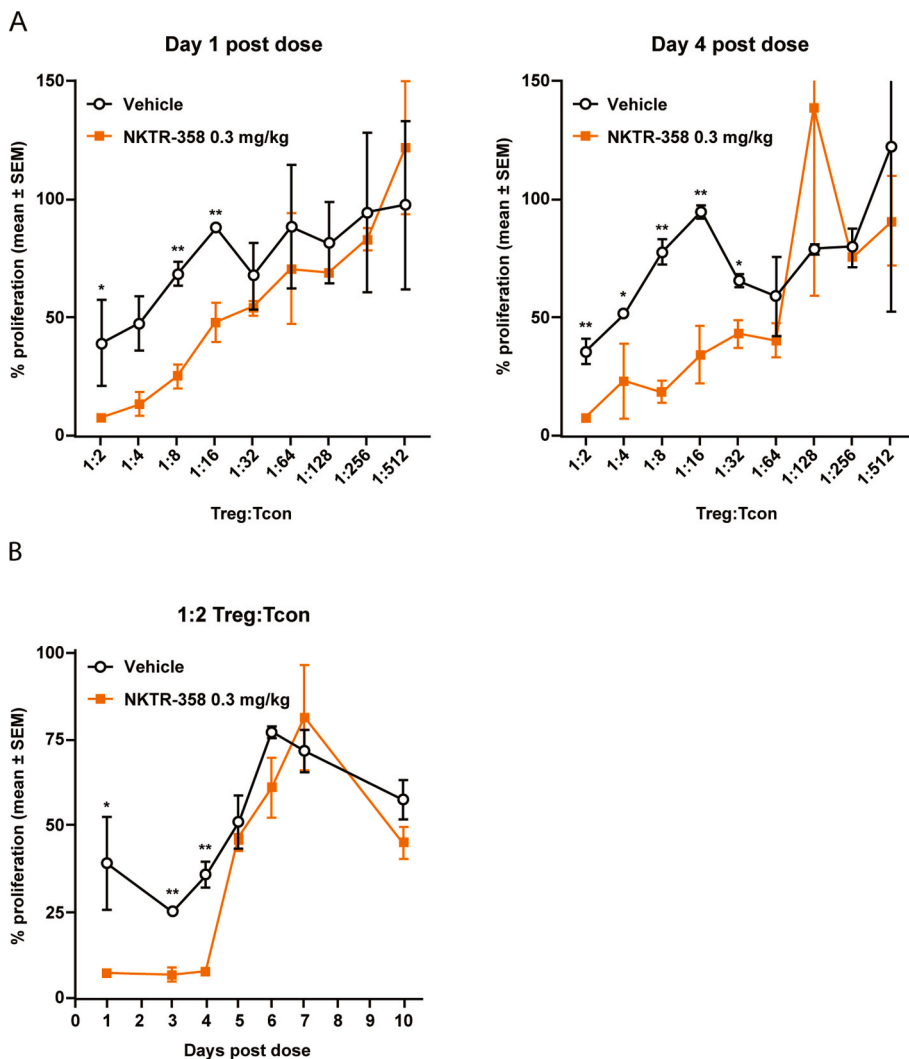


Fig. 5. NKTR-358 increases Treg immunosuppressive activity. Female C57BL/6 mice were administered a single subcutaneous dose of vehicle or NKTR-358 (0.3 mg/kg). Spleens were harvested at indicated days post-dose, and CD4⁺CD25⁺ Tregs were isolated from NKTR-358- or vehicle-treated animals. Tcons were also isolated from mouse spleens harvested from untreated animals. (A) The suppressive capacity of Tregs was assessed following the 72 h co-culture of Tregs and Tcons at different ratios (Treg:Tcon ratios of 1:2 to 1:512) in a standardized [³H]-thymidine uptake assay, and CPM were normalized to % maximal proliferation. A 2-tailed unpaired *t*-test was used to compare differences between treated and control groups at individual Treg:Tcon post-dose. **p* < 0.05; ***p* < 0.01. (B) The relative Treg suppressive capacity of isolated Tregs cultured with Tcons at a Treg:Tcon ratio of 1:2 was assessed over time. A 2-tailed unpaired *t*-test was used to compare differences between treated and control groups at individual times post-dose. **p* < 0.05; ***p* < 0.01. SEM, standard error of the mean; Tcon, conventional T cell; Treg, regulatory T cells.

2-tailed unpaired *t*-test) for Tregs isolated 4 days after dosing. These results strongly demonstrate enhanced Treg potency following NKTR-358 stimulation. The relative suppressive capacity of isolated Tregs at a Treg:Tcon ratio of 1:2 was also assessed on multiple days following subcutaneous administration (Fig. 5B). A single dose of NKTR-358 led to significantly enhanced Treg suppressive activity relative to vehicle treatment for up to 4 days post dose (*p* < 0.05, 2-tailed unpaired *t*-test) before returning to control levels on day 5.

3.7. NKTR-358 leads to preferential and sustained expansion of Tregs in non-human primates

To understand how NKTR-358 functions in a higher species, we next demonstrated the ability of NKTR-358 to selectively mediate *in vivo* Treg expansion and activation as compared with rhIL-2 in cynomolgus monkeys. Flow cytometric immunophenotyping of peripheral blood from cynomolgus monkeys was conducted at various time points before and after either a single subcutaneous administration of NKTR-358 (25 μg/kg), or five consecutive daily subcutaneous doses of rhIL-2 (5 μg/kg/day, totaling 25 μg/kg) (Fig. 6A). Tregs, but not CD8⁺ T cells, showed a robust increase after NKTR-358 administration, starting on day 2 after dosing, peaking on day 7 (more than 15-fold over baseline) and remaining elevated until at least day 14. Daily rhIL-2 treatment over 5 days elicited a modest expansion (~3-fold over baseline) in Tregs that peaked and

resolved earlier compared with the response to NKTR-358. Expansion of Tregs by NKTR-358 was associated with a corresponding and kinetically similar increase in biomarkers of Treg proliferation (Ki67) and activation (CD25), both demonstrating a peak increase of approximately 2-fold over the rhIL-2 response (Fig. 6A). The effect on Treg expansion with NKTR-358 may be attributed to its PK profile in which, following a single 25-μg/kg dose, NKTR-358 reached mean maximum plasma concentrations (*C*_{max}) of 0.25 ng/mL 2 days post-administration and exhibited a long half-life of 10.4 days (Fig. 6B). Expansion of Tregs by NKTR-358 and the corresponding Treg proliferation (Ki67) and activation (CD25) appeared to follow the concentration–time profile of the agent.

IL-2 administration is known to elevate IL-5 levels, which drives mobilization and expansion of eosinophils; an undesirable effect for the treatment of autoimmune and inflammatory disease. Thus, IL-5 and eosinophils levels were compared in the monkeys on day 14 following a single 25-μg/kg subcutaneous dose of NKTR-358 and five daily 5-μg/kg/day subcutaneous administrations of rhIL-2 (Fig. 6C and D). IL-5 levels were undetectable with NKTR-358 treatment, and there was an 8.3-fold lower eosinophil count in NKTR-358-treated animals (0.055 × 10⁶ cells/mL, which is similar to the baseline counts as reported in the literature [37]) compared with rhIL-2-treated monkeys (0.455 × 10⁶ cells/mL). These data support the premise that NKTR-358 does not impact eosinophil expansion at pharmacologically relevant doses.

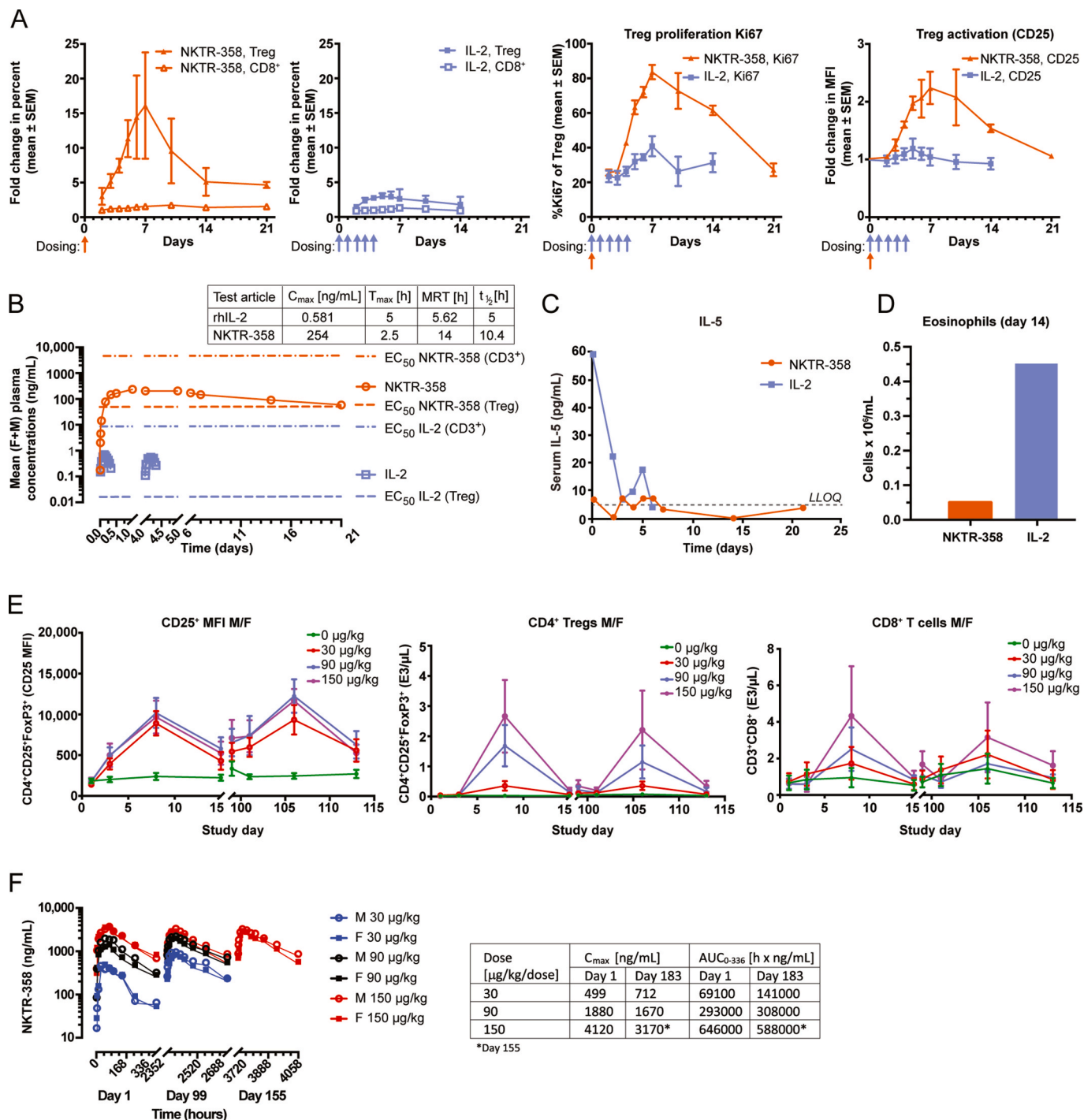


Fig. 6. NKTR-358 promotes preferential expansion of Treg in non-human primates. (A) Two pairs of cynomolgus monkeys (one male and one female per group) received either a single subcutaneous dose of NKTR-358 (25 µg/kg) or five sequential, daily subcutaneous doses of IL-2 (5 µg/kg/day). Blood samples were analyzed for markers of Treg proliferation and activation after gating on lymphocytes. (B) Cynomolgus monkeys (1 F + 1 M) received a single SC dose (25 µg/kg) of NKTR-358 or five SC doses of 5 µg/kg/day (total of 25 µg/kg) of IL-2 and mean plasma concentrations of IL-2 was determined. The EC₅₀ values are derived from Table 2. (C) Serum samples collected for IL-5 quantification were analyzed using LEGENDplex™ and fluorescence intensity was quantified on a flow cytometer. (D) Eosinophils were counted on day 14 post first dosing. Mean eosinophil counts were 0.055 × 10⁶ cell/mL and 0.455 × 10⁶ cells/mL for NKTR-358- and rhIL-2-dosed animals, respectively. (E) and (F). Cynomolgus monkeys (3–7/sex/group) received subcutaneous dose of NKTR-358 at 0 (vehicle control), 30, 90, or 150 µg/kg once every other week (biweekly) for 6 months. Blood samples were collected at various timepoints and used for measurement of CD25⁺ MFI on Tregs, CD4⁺ and CD8⁺ T cells and plasma was used for pharmacokinetics measurements. AUC, area under the curve; C_{max}, maximum plasma concentration; EC₅₀, half maximal effective concentration; F, female; LLOQ, lower limit of quantification; M, male; MFI, mean fluorescence intensity; MRT, mean residence time; SC, subcutaneous; t_{1/2}, half life; T_{max}, time to C_{max}; Tregs, regulatory T cells.

Repeated biweekly subcutaneous dosing of NKTR-358 for 6 months in cynomolgus monkeys demonstrated cyclic increases in the MFI of CD25 on Tregs (Fig. 6E) following each dose (~2-fold increase on day 8, compared with day 3), with the MFI decreasing on day 15 but remaining higher than controls. The MFI of FoxP3 on Tregs was also noted to increase on day 3 of the dosing phase, with similar increases noted on day 8 of the dosing phase in animals administered ≥ 30 $\mu\text{g}/\text{kg}/\text{dose}$, compared with controls (data not shown). The increase in Treg cell numbers and the magnitude of increase in CD25 MFI remained the same following repeat doses (Fig. 6E). Dose-dependent increases in CD8⁺ cells were observed following a similar time course. However, this increase was much lower than the increase in absolute counts of Tregs, with a 4.5-fold vs an 85.8-fold increase for CD8⁺ cells and Tregs, respectively, on day 8 at 150 $\mu\text{g}/\text{kg}$ (≈ 6 x the proposed highest clinical dose) compared with concurrent controls. At 30 $\mu\text{g}/\text{kg}$ (1.5 x the proposed highest clinical dose), there were no appreciable changes in CD8⁺ cell counts, while Tregs increased significantly (>6 x more than vehicle control). Similarly, dose-dependent increases in NK cell counts were also observed with the maximum increase of 3.5-fold observed only at the 150- $\mu\text{g}/\text{kg}$ dose over controls (data not shown). Exposure, as assessed by NKTR-358 mean C_{max} and AUC values, generally increased with the increase in NKTR-358 dose. Weak to moderate accumulation of NKTR-358 was observed after multiple doses in monkeys at the 30- $\mu\text{g}/\text{kg}$ dose while no accumulation was observed after multiple doses at the 90- and 150- $\mu\text{g}/\text{kg}$ doses (Fig. 6F). Over 6 months of repeated dosing, all samples collected for anti-drug antibody analysis were negative (data not shown), indicating that NKTR-358 does not induce immunogenicity while maintaining its pharmacologic effects over time.

3.8. NKTR-358 limits disease development and progression in a murine model of systemic lupus erythematosus

To extend our findings that NKTR-358 promotes Treg proliferation and activation in a manner potentially beneficial for treatment of autoimmune disease, we investigated whether NKTR-358 treatment had an effect on disease development and progression in the murine MRL/MpJ-Fas^{lpr}/MpJ-Fas^{lpr} model of SLE [38].

As expected, MRL/MpJ-Fas^{lpr} mice treated with vehicle alone over 12 weeks developed a systemic autoimmune syndrome that shares features with human SLE, including increased protein levels in the urine; higher BUN; higher serum levels of anti-dsDNA antibodies; and higher kidney histology scores (Fig. 7). Vehicle-treated control mice (C57BL/6) remained healthy and exhibited no SLE-like symptoms.

In contrast, when MRL/MpJ-Fas^{lpr} mice were treated with NKTR-358 at 0.3 mg/kg twice weekly over 12 weeks, urine protein levels remained similar to those in healthy control mice (Fig. 7). NKTR-358 administered at 0.3 mg/kg significantly increased CD4⁺CD25⁺FoxP3⁺ Tregs as a proportion of lymphocyte counts compared with vehicle alone ($p < 0.0001$). Consistent with the effect on Treg expansion, plasma levels of BUN and anti-dsDNA antibodies, as well as kidney histology scores ($p < 0.05$), were also reduced at week 20 in MRL/MpJ-Fas^{lpr} mice treated with 0.3 mg/kg NKTR-358 compared with vehicle. A lower, 0.03-mg/kg dose showed no treatment effect, with increases in urine protein, BUN, and anti-dsDNA antibodies similar to vehicle-treated MRL/MpJ-Fas^{lpr} mice (Fig. 7). A lack of Treg proliferation in the 0.03-mg/kg dose group correlated with the absence of treatment effect.

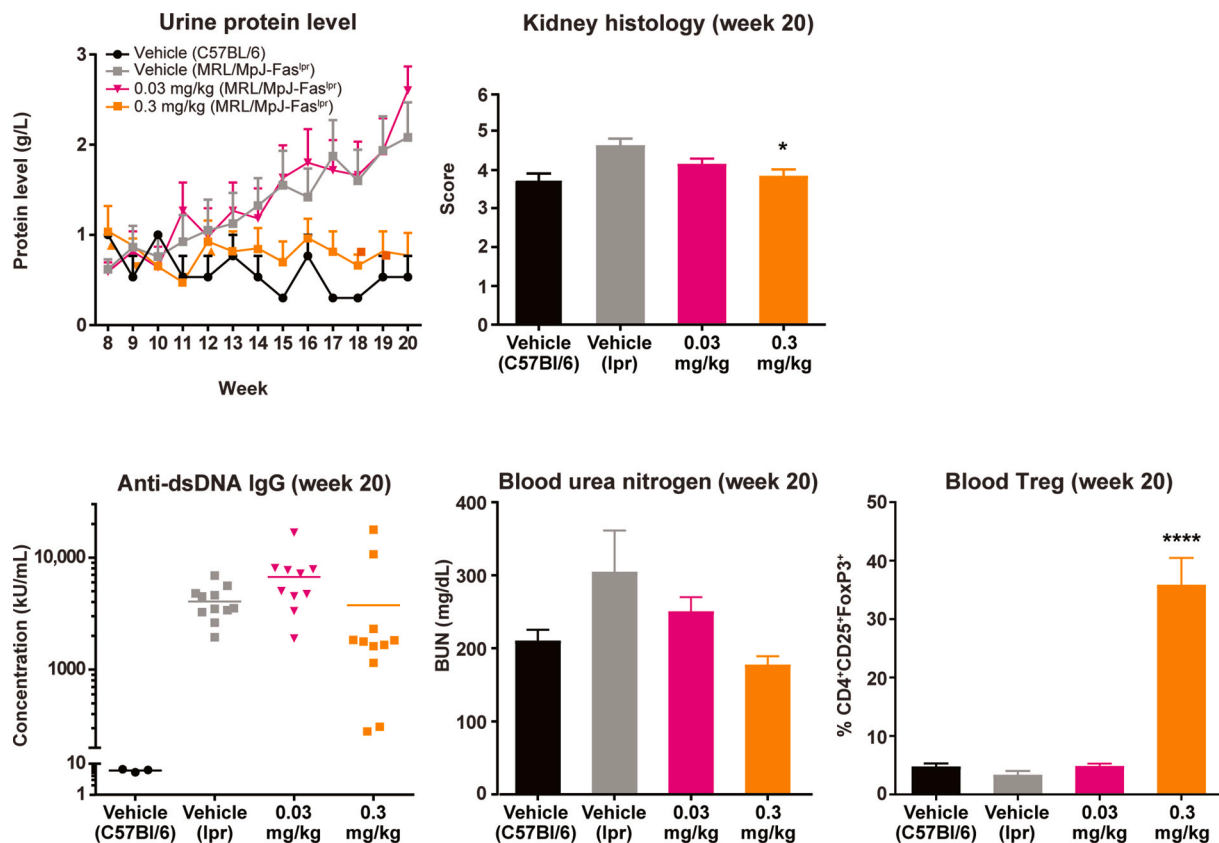


Fig. 7. NKTR-358 is efficacious in a mouse model of SLE. Three groups of 15 MRL/MpJ-Fas^{lpr} mice were treated with vehicle or NKTR-358 at 0.03 or 0.3 mg/kg twice weekly for 12 weeks after an 8-week baseline period. A control group of three C57BL/6 mice received vehicle alone on the same dosing schedule. Urine was collected at baseline and weekly for protein analysis. Blood samples collected at baseline and at week 20 were analyzed for anti-dsDNA antibodies, blood urea nitrogen, and Treg populations. Kidney histology were evaluated at week 20. * $p < 0.05$; **** $p < 0.0001$. BUN, blood urea nitrogen; dsDNA, double-stranded DNA; IgG, immunoglobulin G; SLE, systemic lupus erythematosus; Treg, regulatory T cell.

4. Discussion

The biological functions of IL-2 are pleiotropic with opposing mechanisms of action in different T-cell subsets, based on a difference in IL-2 receptor biology between Tcons and Tregs [1]. At high concentrations, IL-2 induces expansion of CD8⁺ effector and memory CTLs and NK cells through the intermediate-affinity $\beta\gamma$ receptor [4] which lends to its antitumor activity [5–7]. In contrast, low concentrations of IL-2 act through the high-affinity $\alpha\beta\gamma$ receptor to expand and activate Tregs [4]. Hence, IL-2 at low doses can preferentially expand Tregs in conditions of relative Treg deficiency (e.g. autoimmunity and chronic inflammatory conditions). NKTR-358 is a pharmacologically active PEGylated rhIL-2 that has a markedly prolonged half-life compared to rhIL-2. In this study, we have shown by a variety of measures and across species, that NKTR-358 induces sustained, selective proliferation and activation of Tregs with minimal effect on Tcons. We demonstrated that a single dose of NKTR-358 shows improved PD and prolonged PK compared with the same total dose of rhIL-2 and that NKTR-358 can be dosed repeatedly over a 6-month period in non-human primates with no loss of activity over the duration of treatment. NKTR-358 induces functional Tregs capable of robust suppressive activity and has the ability to reduce pathological markers associated with disease progression in a murine model of SLE.

NKTR-358 was discovered through an *in vivo* screening process in mice, designed to identify a molecule that selectively induced Tregs. NKTR-358 was thus selected for optimal *in vivo* biological properties prior to biochemical and biophysical analysis. NKTR-358 administration exhibited dose-dependent increases in Tregs *in vivo* in mice, with minimal changes in CD8⁺ T cells and NK cells. In-depth characterization of the IL-2 receptor affinity demonstrated that NKTR-358 has reduced on-rates for IL-2R α , IL-2R β , and IL-2R $\alpha\beta$ compared with rhIL-2, with minimal differences in off-rates. The biological consequence of significantly reduced affinity of NKTR-358 to IL-2R β is likely the minimal activation of cells that express the low-affinity IL-2R $\beta\gamma$, such as Tcons. In contrast, the diminished but retained affinity for IL-2R α and IL-2R $\alpha\beta$ would favor engagement of cells expressing the high-affinity trimeric IL-2R $\alpha\beta\gamma$, which is present on Tregs, leading to preferential activity of this cell subset. Treg activation occurs at low IL-2 concentrations [4], and we have demonstrated that NKTR-358 can achieve a phosphorylated STAT5 EC₅₀ in Tregs that is well below the EC₅₀ in Tcons. Despite NKTR-358's attenuated potency compared with rhIL-2, and the corresponding rightward shift in the concentration–response curves for *in vitro* pSTAT5 induction in Tregs and CD8⁺ T cells, maximal pharmacological response (efficacy) was preserved. NKTR-358's extremely long half-life (10.4 days) likely also contributed to the preserved *in vivo* potency in Treg activation, despite decreased receptor binding. Despite attenuated receptor binding and administration at a lower dose, the exposure and magnitude of Treg increase were much higher with NKTR-358 compared with IL-2.

We used ICOS expression as a biomarker of activation in Tregs. After a single dose of NKTR-358, the expanded Treg population in mice exhibited a proliferative (Ki67⁺) and activated (ICOS⁺) phenotype. Ki67⁺ Treg populations increased 2-fold from day 2 to day 6, and the percentage of ICOS⁺ Tregs was elevated compared with control animals from day 2 to day 4. The time course of this proliferative and activated Treg phenotype aligns with our observations on the duration of the Tregs' immunosuppressive activity *ex vivo*. Tregs isolated from NKTR-358-treated mice exhibited dose- and time-dependent enhanced capacity for inhibiting Tcons at Treg:Tcon ratios as low as 1:8, with the strongest effects observed between 1 and 4 days following a single dose. In contrast, Tregs from vehicle-treated mice only exhibited basal suppressive capability, with maximal suppression at a Treg:Tcon ratio of 1:2. Thus, the proliferative and activated phenotype of the NKTR-358-induced Tregs observed *in vivo* translates to *ex vivo* immunosuppressive activity.

We have used the expression of Helios and neuropilin-1 to

demonstrate that NKTR-358 induces both nTreg-like and pTreg-like cells. NKTR-358 induced a similar increase in Tregs in both normal and thymectomized mice. This suggested that the Tregs that were induced in the thymectomized mice were pTreg, resulting from CD4⁺ cells that had differentiated outside the thymus, and this was further supported by these Tregs exhibiting a decrease in Helios⁺ staining. Normal mice had a substantial increase in Helios⁺ Tregs (nTregs). Conflicting evidence exists as to whether Helios is a specific marker for thymic-derived Tregs or if additional markers should be used to further identify these distinct Treg populations [39,40]. Neuropilin-1, a semaphorin III receptor, is used as a marker for thymic Tregs under certain conditions [41–43]. We evaluated neuropilin-1 expression on Tregs and demonstrated that NKTR-358 induced high levels of nTreg-like cells as well as lower levels of pTreg-like cells, strengthening the overall observation that NKTR-358 can expand both Treg populations. Overall, by evaluating Helios and neuropilin-1 expression on Tregs we have shown that while the majority of Tregs that are induced by NKTR-358 are of thymic origin, with a 3:1 ratio of nTreg:pTreg, NKTR-358 can also promote induction of pTregs, as demonstrated by the induction of Tregs in thymectomized mice.

Treatment of non-human primates showed that a single NKTR-358 dose (25 $\mu\text{g}/\text{kg}$) preferentially stimulated the proliferation and activation of Tregs without a corresponding increase in Tcons. This response was stronger and more durable than that elicited by five daily doses of rhIL-2 (5 $\mu\text{g}/\text{kg}/\text{day}$). Previous clinical studies in humans reported Treg expansion following the administration of rhIL-2 in doses ranging from 1 million IU every other day to 1.5 million IU daily [18,44,45]. Assuming an average adult weight of 70 kg and using the conversion factor provided in the manufacturer's label, rhIL-2 doses used in human studies were up to 1.3 $\mu\text{g}/\text{kg}/\text{day}$. Hence, the rhIL-2 dose of 5 $\mu\text{g}/\text{kg}/\text{day}$ used in our study of non-human primates was more than adequate to elicit the clinically relevant Treg proliferation response possible with this agent. Despite this, the increase in the Treg population with rhIL-2 was modest (3-fold over baseline). In contrast, a single dose of NKTR-358 (25 $\mu\text{g}/\text{kg}$) increased Tregs by more than 15-fold over baseline, peaking at 7 days and remaining elevated until at least day 14, while the change in Tcons was minimal. Furthermore, repeated dosing of NKTR-358 over 6 months led to similar increases in Treg numbers and CD25 MFI following each dose. Overall, the improved and differentiated PK/PD profile of NKTR-358 over rhIL-2 leads to its ability to promote stronger and more durable Treg induction and proliferation.

NKTR-358's selectivity for Treg proliferation and activation makes it a promising potential therapeutic candidate for treating autoimmune inflammatory diseases associated with T-cell dysfunction, such as SLE. This autoimmune inflammatory disease affects mostly middle-aged women, and its characteristic symptoms include skin eruptions, joint pain, recurrent pleurisy, and kidney disease [46]. The ability of NKTR-358 to alleviate some of the hallmark pathologies of SLE was tested using the most commonly studied mouse model of the disease (MRL/MpJ-Fas^{lpr} mice) [47]. These mice develop an autoimmune disease that reflects pathologies of human SLE, including lymph node enlargement, increased immunoglobulin G levels, antinuclear antibody production, proteinuria, and kidney failure caused by inflammation of the glomeruli. NKTR-358 administration in MRL/MpJ-Fas^{lpr} mice led to dose-dependent reduction in several pathological markers of SLE. When administered to MRL/MpJ-Fas^{lpr} mice at 0.3 mg/kg twice-weekly over 12 weeks, NKTR-358 led to reduction in several pathological markers of SLE (e.g. urine protein level, BUN, and anti-dsDNA antibodies), accompanied by an increase in Tregs, as compared with MRL/MpJ-Fas^{lpr} mice treated with vehicle alone.

Previous studies have demonstrated the potential for low-dose rhIL-2 to expand Tregs *in vivo* [4,44,48], but to date, there is no approved therapeutic that can yet fulfill the clinical need for a long-acting, effective IL-2 pathway agonist for treatment of inflammatory and autoimmune disease. A 2015 report by Bell and colleagues describes efforts to develop two rhIL-2 analogs engineered for long half-life

through the covalent attachment of a non-FcR γ binding human IgG1 [49]. Compared with rhIL-2, single doses of the rhIL-2–IgG1 fusion proteins in non-human primates did indeed elicit durable responses associated with sustained pSTAT5 induction and increases in CD25, Foxp3, and Ki67 expression, without symptoms of eosinophilia. These results are consistent with the results observed in the present study and support the hypothesis that modifications to extend the half-life of rhIL-2 may have potential benefits.

NKTR-358 may have advantages compared with other rhIL-2 analogs in development [49,50]. There have been various attempts at alteration of rhIL-2 to improve Treg selectivity and half-life, including mutant IL-2, IL-2 fusion proteins, and anti-IL-2 antibodies [49–51]. NKTR-358 utilizes the approved rhIL-2 aldesleukin sequence rather than a mutein thereof or a fusion protein, and is not an antibody-based therapy, and thus has minimal potential for the development of anti-drug antibodies that may decrease clinical effectiveness over time. Indeed, in our non-human primate study, no anti-drug antibodies were detected during 6 months of NKTR-358 administration.

This study bears the common limitations of preclinical and animal studies. Experiments in whole blood, mouse models, and non-human primate models are essential for establishing basic mechanisms and PK/PD and functional assessments. While the science behind these preclinical models is well established, data from these experiments are subject to the biological differences between animal and human physiology. As is standard for mechanistic studies, female mice were used as male mice are more aggressive, which in turn can impact immune response. However, mouse gender differences in IL-2-driven immune responses are unlikely and studies in cynomolgus monkeys did not reveal any differences. Initial clinical experience with NKTR-358 was recently presented [52] and aligns with the preclinical data presented here. In healthy volunteers, single ascending doses of NKTR-358 showed selective and dose-dependent expansion of Tregs for more than 20 days after a single dose, without measurable changes in percentages or numbers of CD4⁺ and CD8⁺ T cells and only low-level increases in NK cell numbers at the highest doses studied. NKTR-358 was recently studied in a Phase Ib trial in patients with SLE (NCT033556007) and is currently being studied in patients with psoriasis (NCT04119557) and eczema (NCT04081350).

5. Conclusions

Our results show that NKTR-358 can elicit sustained and preferential proliferation and activation of Tregs in human whole blood, mouse models, and non-human primates, without corresponding increases in CD8⁺ T cells. A single dose of NKTR-358 in cynomolgus monkeys resulted in sustained activity that lasted for at least 14 days compared with the transient response in rhIL-2 treated animals. Repeated NKTR-358 doses over 6 months demonstrated expansion of Tregs following each dose. Importantly, no anti-drug antibodies were detected during the 6 months of dosing. Functionally, the Treg-selective PD properties of NKTR-358 were consistent with its ability to suppress Tcons in an *ex vivo* proliferation assay and to suppress the development of T-cell-mediated autoimmune pathology in a mouse model of SLE.

Additional studies to assess this molecule's potential as a therapy for autoimmune diseases are underway. A single dose Phase I study of NKTR-358 in healthy human subjects was conducted, which evaluated Treg mobilization, functional activity, PK, and safety. Subsequently, a multiple ascending dose trial in patients with SLE has also recently been completed (NCT03556007).

Funding

The study was funded by Nektar Therapeutics. Nektar will consider requests for access to NKTR-358 from qualified researchers for non-clinical research purposes. Requests should be made to the corresponding author.

Declaration of competing interest

The authors declare the following financial interests/personal relationships which may be considered as potential competing interests. All authors, except JR and YK, were employees and shareholders of Nektar Therapeutics during this study. JR reports research funding from Amgen, Equillum, and Kite Pharma and consulting income from Aleta Biotherapeutics, AvroBio, Celgene, Falcon Therapeutics, LifeVault Bio, Rheos Medicines, Tal, and TScan Therapeutics. YK has no known competing financial interests or personal relationships that could have appeared to influence the work reported in this paper.

Acknowledgments

The authors thank Phillips-Gilmore Oncology Communications, Jeanne McAdara, PhD, and Kai I. Cheang, PharmD, MS, for professional assistance with manuscript preparation and Mark Hardy of BOLDS-CIENCE for professional assistance with figure development.

Appendix A. Supplementary data

Supplementary data to this article can be found online at <https://doi.org/10.1016/j.jtauto.2021.100103>.

References

- [1] O. Boyman, J. Sprent, The role of interleukin-2 during homeostasis and activation of the immune system, *Nat. Rev. Immunol.* 12 (2012) 180–190, <https://doi.org/10.1038/nri3156>.
- [2] T.R. Malek, I. Castro, Interleukin-2 receptor signaling: at the interface between tolerance and immunity, *Immunity* 33 (2010) 153–165, <https://doi.org/10.1016/j.immuni.2010.08.004>.
- [3] W. Liao, J.-X. Lin, W. Leonard, IL-2 family cytokines: new insights into the complex roles of IL-2 as a broad regulator of T helper cell differentiation, *Curr. Opin. Immunol.* 23 (2011) 598–604.
- [4] E. Zorn, E.A. Nelson, M. Mohseni, F. Porcheray, H. Kim, D. Litsa, et al., IL-2 regulates FOXP3 expression in human CD4⁺CD25⁺ regulatory T cells through a STAT-dependent mechanism and induces the expansion of these cells *in vivo*, *Blood* 108 (2006) 1571–1579, <https://doi.org/10.1182/blood-2006-02-004747>.
- [5] R. Setoguchi, S. Hori, T. Takahashi, S. Sakaguchi, Homeostatic maintenance of natural Foxp3(+) CD25(+) CD4(+) regulatory T cells by interleukin (IL)-2 and induction of autoimmune disease by IL-2 neutralization, *J. Exp. Med.* 201 (2005) 723–735, <https://doi.org/10.1084/jem.20041982>.
- [6] K. Ohl, K. Tenbrock, Regulatory T cells in systemic lupus erythematosus, *Eur. J. Immunol.* 45 (2015) 344–355, <https://doi.org/10.1002/eji.201344280>.
- [7] H. Yang, W. Zhang, L. Zhao, Y. Li, F. Zhang, F. Tang, et al., Are CD4⁺CD25⁺Foxp3⁺ cells in untreated new-onset lupus patients regulatory T cells? *Arthritis Res. Ther.* 11 (2009) R153, <https://doi.org/10.1186/ar2829>.
- [8] D. Busse, M. de la Rosa, K. Hobiger, K. Thurley, M. Flossdorf, A. Scheffold, et al., Competing feedback loops shape IL-2 signaling between helper and regulatory T lymphocytes in cellular microenvironments, *Proc. Natl. Acad. Sci. U. S. A.* 107 (2010) 3058–3063, <https://doi.org/10.1073/pnas.0812851107>.
- [9] P.E. Kintzel, K.A. Calis, Recombinant interleukin-2: a biological response modifier, *Clin. Pharm.* 10 (1991) 110–128.
- [10] R.P. Whitehead, D. Ward, L. Hemingway, G.P. Hemstreet, E. Bradley, M. Konrad, Subcutaneous recombinant interleukin 2 in a dose escalating regimen in patients with metastatic renal cell adenocarcinoma, *Cancer. Res.* 50 (1990) 6708–6715.
- [11] G.C. Sim, L. Radvanyi, The IL-2 cytokine family in cancer immunotherapy, *Cytokine. Growth. Factor. Rev* 25 (2014) 377–390, <https://doi.org/10.1016/j.cytogr.2014.07.018>.
- [12] D. Klatzmann, A.K. Abbas, The promise of low-dose interleukin-2 therapy for autoimmune and inflammatory diseases, *Nat. Rev. Immunol.* 15 (2015) 283–294, <https://doi.org/10.1038/nri3823>.
- [13] J. Koreth, H.T. Kim, K.T. Jones, P.B. Lange, C.G. Reynolds, M.J. Chammas, et al., Efficacy, durability, and response predictors of low-dose interleukin-2 therapy for chronic graft-versus-host disease, *Blood* 128 (2016) 130–137, <https://doi.org/10.1182/blood-2016-02-702852>.
- [14] D. Saadoun, M. Rosenzweig, F. Joly, A. Six, F. Carrat, V. Thibault, et al., Regulatory T-cell responses to low-dose interleukin-2 in HCV-induced vasculitis, *N. Engl. J. Med.* 365 (2011) 2067–2077, <https://doi.org/10.1056/NEJMoa1105143>.
- [15] J.Y. Humrich, C. von Spee-Mayer, E. Siebert, T. Alexander, F. Hiepe, A. Radbruch, et al., Rapid induction of clinical remission by low-dose interleukin-2 in a patient with refractory SLE, *Ann. Rheum. Dis.* 74 (2015) 791–792, <https://doi.org/10.1136/annrheumdis-2014-206506>.
- [16] J. He, R. Zhang, M. Shao, X. Zhao, M. Miao, J. Chen, et al., Efficacy and safety of low-dose IL-2 in the treatment of systemic lupus erythematosus: a randomised, double-blind, placebo-controlled trial, *Ann. Rheum. Dis.* 79 (2020) 141–149, <https://doi.org/10.1136/annrheumdis-2019-215396>.

- [17] J.A. Todd, M. Evangelou, A.J. Cutler, M.L. Pekalski, N.M. Walker, H.E. Stevens, et al., Regulatory T cell responses in participants with type 1 diabetes after a single dose of interleukin-2: a non-randomised, open label, adaptive dose-finding trial, *PLoS Med.* 13 (2016), e1002139, <https://doi.org/10.1371/journal.pmed.1002139>.
- [18] M. Rosenzweig, R. Lorenzon, P. Cacoub, H.P. Pham, F. Pitoiset, K. El Soufi, et al., Immunological and clinical effects of low-dose interleukin-2 across 11 autoimmune diseases in a single, open clinical trial, *Ann. Rheum. Dis.* 78 (2019) 209–217, <https://doi.org/10.1136/annrheumdis-2018-214229>.
- [19] M.W. Konrad, G. Hemstreet, E.M. Hersh, P.W. Mansell, R. Mertelsmann, J.E. Kolitz, et al., Pharmacokinetics of recombinant interleukin 2 in humans, *Cancer Res* 50 (1990) 2009–2017.
- [20] S.-E. Bentebibel, M.E. Hurwitz, C. Bernatchez, C. Haymaker, C.W. Hudgens, H. M. Kluger, et al., A first-in-human study and biomarker analysis of NKTR-214, a novel IL2 β -biased cytokine, in patients with advanced or metastatic solid tumors, *Canc. Discov.* 9 (2019) 711–721, <https://doi.org/10.1158/2159-8290.CD-18-1495>.
- [21] D.H. Charych, U. Hoch, J.L. Langowski, S.R. Lee, M.K. Addepalli, P.B. Kirk, et al., NKTR-214: an engineered cytokine with biased IL2 receptor binding, increased tumor exposure, and marked efficacy in mouse tumor models, *Clin. Canc. Res.* 22 (2016) 680–690, <https://doi.org/10.1158/1078-0432.CCR-15-1631>.
- [22] D. Charych, S. Khalili, V. Dixit, P. Kirk, T. Chang, J. Langowski, et al., Modeling the receptor pharmacology, pharmacokinetics, and pharmacodynamics of NKTR-214, a kinetically-controlled interleukin-2 (IL2) receptor agonist for cancer immunotherapy, *PLoS One* 12 (2017), e0179431, <https://doi.org/10.1371/journal.pone.0179431>.
- [23] M. Hirakawa, T. Matos, H. Liu, J. Koreth, H.T. Kim, N.E. Paul, et al., Low-dose IL-2 selectively activates subsets of CD4⁺ Tregs and NK cells, *JCI Insight* 1 (2016), e89278, <https://doi.org/10.1172/jci.insight.89278>.
- [24] S.C. Bendall, E.F. Simonds, P. Qiu, E.D. Amir, P.O. Krutzik, R. Finck, et al., Single-cell mass cytometry of differential immune and drug responses across a human hematopoietic continuum, *Science* 332 (2011) 687–696, <https://doi.org/10.1126/science.1198704>.
- [25] E.D. Amir, K.L. Davis, M.D. Tadmor, E.F. Simonds, J.H. Levine, S.C. Bendall, et al., viSNE enables visualization of high dimensional single-cell data and reveals phenotypic heterogeneity of leukemia, *Nat. Biotechnol.* 31 (2013) 545–552, <https://doi.org/10.1038/nbt.2594>.
- [26] M.A. Cheever, J.A. Thompson, D.E. Kern, P.D. Greenberg, Interleukin 2 (IL 2) administered in vivo: influence of IL 2 route and timing on T cell growth, *J. Immunol.* 134 (1985) 3895–3900.
- [27] S. Hori, T. Takahashi, S. Sakaguchi, Control of autoimmunity by naturally arising regulatory CD4⁺ T cells, *Adv. Immunol.* 81 (2003) 331–371, [https://doi.org/10.1016/s0065-2776\(03\)81008-8](https://doi.org/10.1016/s0065-2776(03)81008-8).
- [28] J.D. Fontenot, M.A. Gavin, A.Y. Rudensky, Foxp3 programs the development and function of CD4⁺CD25⁺ regulatory T cells, *Nat. Immunol.* 4 (2003) 330–336, <https://doi.org/10.1038/ni904>.
- [29] S. Sakaguchi, N. Sakaguchi, M. Asano, M. Itoh, M. Toda, Immunologic self-tolerance maintained by activated T cells expressing IL-2 receptor α -chains (CD25). Breakdown of a single mechanism of self-tolerance causes various autoimmune diseases, *J. Immunol.* 155 (1995) 1151–1164.
- [30] Z. Li, D. Li, A. Tsun, B. Li, FOXP3⁺ regulatory T cells and their functional regulation, *Cell. Mol. Immunol.* 12 (2015) 558–565, <https://doi.org/10.1038/cmi.2015.10>.
- [31] M. Kornete, E. Sgouroudis, C.A. Piccirillo, ICOS-dependent homeostasis and function of Foxp3⁺ regulatory T cells in islets of nonobese diabetic mice, *J. Immunol.* 188 (2012) 1064–1074, <https://doi.org/10.4049/jimmunol.1101303>.
- [32] L. Strauss, C. Bergmann, M.J. Szczepanski, S. Lang, J.M. Kirkwood, T.L. Whiteside, Expression of ICOS on human melanoma-infiltrating CD4⁺CD25^{high}Foxp3⁺ T regulatory cells: implications and impact on tumor-mediated immune suppression, *J. Immunol.* 180 (2008) 2967–2980, <https://doi.org/10.4049/jimmunol.180.5.2967>.
- [33] K. Wing, Y. Onishi, P. Prieto-Martin, T. Yamaguchi, M. Miyara, Z. Fehervari, et al., CTLA-4 control over Foxp3⁺ regulatory T cell function, *Science* 322 (2008) 271–275, <https://doi.org/10.1126/science.1160062>.
- [34] S. Kumar, S. Malik, U.P. Singh, S. Ponnazhagan, K. Scissum-Gunn, U. Manne, et al., PD-1 expression on Foxp3⁺ Treg cells modulates CD8⁺ T cell function in prostatic tumor microenvironment, *J. Immunol.* 198 (2017), 155.11.
- [35] G. Liao, S. Nayak, J.R. Regueiro, S.B. Berger, C. Detre, X. Romero, et al., GITR engagement preferentially enhances proliferation of functionally competent CD4⁺CD25⁺FoxP3⁺ regulatory T cells, *Int. Immunol.* 22 (2010) 259–270, <https://doi.org/10.1093/intimm/dxq001>.
- [36] C.E. Ruby, M.A. Yates, D. Hirschhorn-Cymerman, P. Chlebeck, J.D. Wolchok, A. N. Houghton, et al., Cutting Edge: OX40 agonists can drive regulatory T cell expansion if the cytokine milieu is right, *J. Immunol.* 183 (2009) 4853–4857, <https://doi.org/10.4049/jimmunol.0901112>.
- [37] A. Wilcox, Reference Intervals for Selected Hematology, Coagulation, and Clinical Chemistry Parameters in Chinese, Mauritian, and Cambodian Cynomolgus Monkeys, Charles River Laboratories International, Inc., 2015.
- [38] J.C. Gutierrez-Ramos, J.L. Andreu, Y. Revilla, E. Viñuela, C. Martinez, Recovery from autoimmunity of MRL/lpr mice after infection with an interleukin-2/vaccinia recombinant virus, *Nature* 346 (1990) 271–274, <https://doi.org/10.1038/346271a0>.
- [39] T. Akimova, U.H. Beier, L. Wang, M.H. Levine, W.W. Hancock, Helios expression is a marker of T cell activation and proliferation, *PLoS One* 6 (2011), e24226, <https://doi.org/10.1371/journal.pone.0024226>.
- [40] M.E. Himmel, K.G. MacDonald, R.V. Garcia, T.S. Steiner, M.K. Levings, Helios⁺ and Helios⁻ cells coexist within the natural FOXP3⁺ T regulatory cell subset in humans, *J. Immunol.* 190 (2013) 2001–2008, <https://doi.org/10.4049/jimmunol.1201379>.
- [4][1] M. Yadav, C. Louvet, D. Davini, J.M. Gardner, M. Martinez-Llordella, S. Bailey-Bucktrout, et al., Neuropilin-1 distinguishes natural and inducible regulatory T cells among regulatory T cell subsets in vivo, *J. Exp. Med.* 209 (2012) 1713–1722, <https://doi.org/10.1084/jem.20120822>. S1–19.
- [4][2] J.M. Weiss, A.M. Bilate, M. Gobert, Y. Ding, M.A. Curotto de Lafaille, C. N. Parkhurst, et al., Neuropilin 1 is expressed on thymus-derived natural regulatory T cells, but not mucosa-generated induced Foxp3⁺ T reg cells, *J. Exp. Med.* 209 (2012) 1723–1742, <https://doi.org/10.1084/jem.20120914>. S1.
- [43] D. Bruder, M. Probst-Keppler, A.M. Westendorf, R. Geffers, S. Beissert, K. Loser, et al., Neuropilin-1: a surface marker of regulatory T cells, *Eur. J. Immunol.* 34 (2004) 623–630, <https://doi.org/10.1002/eji.200324799>.
- [44] J. He, X. Zhang, Y. Wei, X. Sun, Y. Chen, J. Deng, et al., Low-dose interleukin-2 treatment selectively modulates CD4⁺ T cell subsets in patients with systemic lupus erythematosus, *Nat. Med.* 22 (2016) 991–993, <https://doi.org/10.1038/nm.4148>.
- [4][5] J.Y. Humrich, G. Riemekasten, Low-dose interleukin-2 therapy for the treatment of systemic lupus erythematosus, *Curr. Opin. Rheumatol.* 31 (2019) 208–212, <https://doi.org/10.1097/BOR.0000000000000575>.
- [4][6] P.E. Lipsky, Systemic lupus erythematosus: an autoimmune disease of B cell hyperactivity, *Nat. Immunol.* 2 (2001) 764–766, <https://doi.org/10.1038/ni0901-764>.
- [47] O.T. Chan, L.G. Hannum, A.M. Haberman, M.P. Madaio, M.J. Shlomchik, A novel mouse with B cells but lacking serum antibody reveals an antibody-independent role for B cells in murine lupus, *J. Exp. Med.* 189 (1999) 1639–1648, <https://doi.org/10.1084/jem.189.10.1639>.
- [48] S. Ito, C.M. Bollard, M. Carlsten, J.J. Melenhorst, A. Biancotto, E. Wang, et al., Ultra-low dose interleukin-2 promotes immune-modulating function of regulatory T cells and natural killer cells in healthy volunteers, *Mol. Ther.* 22 (2014) 1388–1395, <https://doi.org/10.1038/mt.2014.50>.
- [49] C.J.M. Bell, Y. Sun, U.M. Nowak, J. Clark, S. Howlett, M.L. Pekalski, et al., Sustained in vivo signaling by long-lived IL-2 induces prolonged increases of regulatory T cells, *J. Autoimmun.* 56 (2015) 66–80, <https://doi.org/10.1016/j.jaut.2014.10.002>.
- [50] NCBI MedGen, IL-2 mutein/Fc Fusion Protein AMG 592, NCBI, 2019. <http://www.ncbi.nlm.nih.gov/medgen/1633069>. (Accessed 29 May 2019).
- [5][1] M. Mizui, Natural and modified IL-2 for the treatment of cancer and autoimmune diseases, *Clin. Immunol.* 206 (2019) 63–70, <https://doi.org/10.1016/j.clim.2018.11.002>.
- [52] C. Fanton, S. Siddhanti, N. Dixit, L. Lu, T. Gordi, D. Dickerson, et al., Selective expansion of regulatory T-cells in humans by a novel IL-2 conjugate T-reg stimulator, NKTR-358, being developed for the treatment of autoimmune diseases, in: European League against Rheumatism (EULAR) Annual Meeting, 2019, <https://doi.org/10.1136/annrheumdis-2019-eular.3395>. Oral OP0195.